Drift Prospecting for Porphyry Copper-Gold, Volcanogenic Massive Sulphide Mineralization and Precious and Base Metal Veins within the QUEST Project Area, Central British Columbia (NTS 093J)

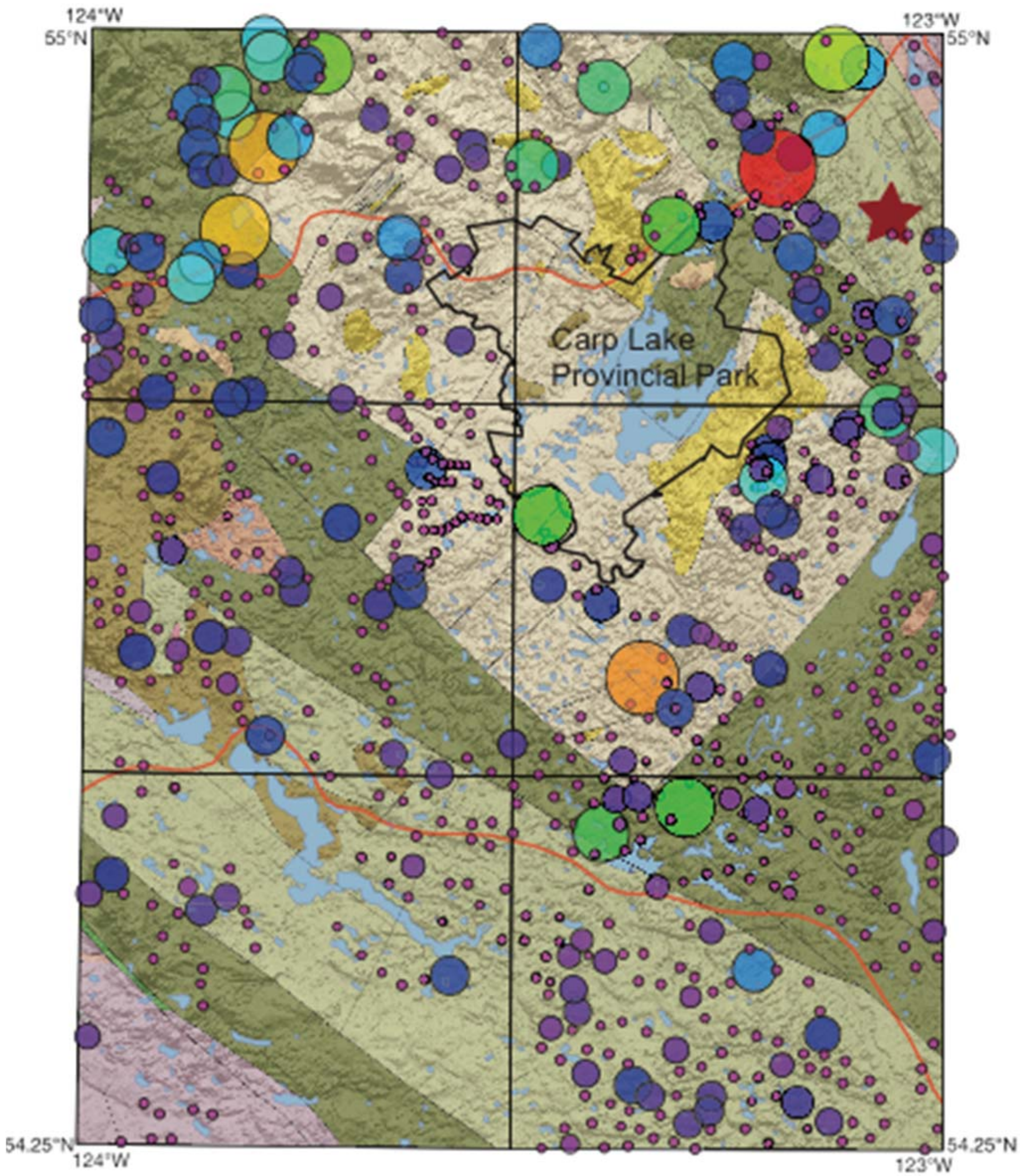

Brent C. Ward, Matthew I. Leybourne, David A. Sacco, Raymond E. Lett, Lambertus C. Struik

Drift Prospecting for Porphyry Copper-Gold, Volcanogenic Massive Sulphide Mineralization and Precious and Base Metal Veins within the QUEST Project Area, Central British Columbia (NTS 093J)

Brent C. Ward[1], Matthew I. Leybourne[2], David A. Sacco[1], Raymond E. Lett[3], Lambertus C. Struik[4]

[1]Department of Earth Sciences, Simon Fraser University, Burnaby, BC V5A 1S6; bcward@sfu.ca
[2]ALS Geochemistry, 2103 Dollarton Hwy, North Vancouver, BC V7H 0A7
[3]BC Geological Survey Emeritus 3956 Ashford Rd, Victoria, BC V8P 3S5
[4]Geological Survey of Canada, Natural Resources Canada, 1500 - 605 Robson Street, Vancouver, BC V6B 5J3

INTRODUCTION

This report summarizes the results of regional till geochemical and mineralogical surveys and Quaternary studies conducted in the heart of the QUEST Project area (Geoscience BC's program to attract new exploration in an under-explored portion of central British Columbia, initiated in 2007; http://www.geosciencebc.com/s/Quest.asp) (Figure 1). The QUEST Project area has good potential for Cu-Au porphyry and volcanogenic massive sulphide (VMS) mineralization, but mineral exploration activity has been hindered in some areas due to the thick cover of surficial deposits. Regional-scale till sampling followed by detailed surveys around samples with elevated or anomalous values was carried out to assess mineral potential of this area. Till is the preferred sampling medium for geochemical and mineralogical surveys in glaciated terrain because it is commonly considered a first derivative of bedrock (Dreimanis, 1989; Levson, 2001). This methodology has been shown to aid in identifying potentially mineralized bedrock units in areas covered with thick glacial deposits (Levson, 2001; McClenaghan et al., 2002; McClenaghan, 2005). The Quaternary geology, specifically the distribution of surficial deposits and the ice-flow history, including the dominant transport direction, were used to plan the surveys and determine the transport history of till geochemical and mineralogical data.

The primary goal of this study is to use regional-scale major-, minor- and trace-element till geochemical data, gold grain counts and heavy mineral separation and identification to identify mineralized bedrock. The geochemical and mineralogical data presented here highlight new exploration targets and, in combination with the area's glacial history, provide a surficial geological context for companies to interpret their own geochemical and bedrock geology datasets.

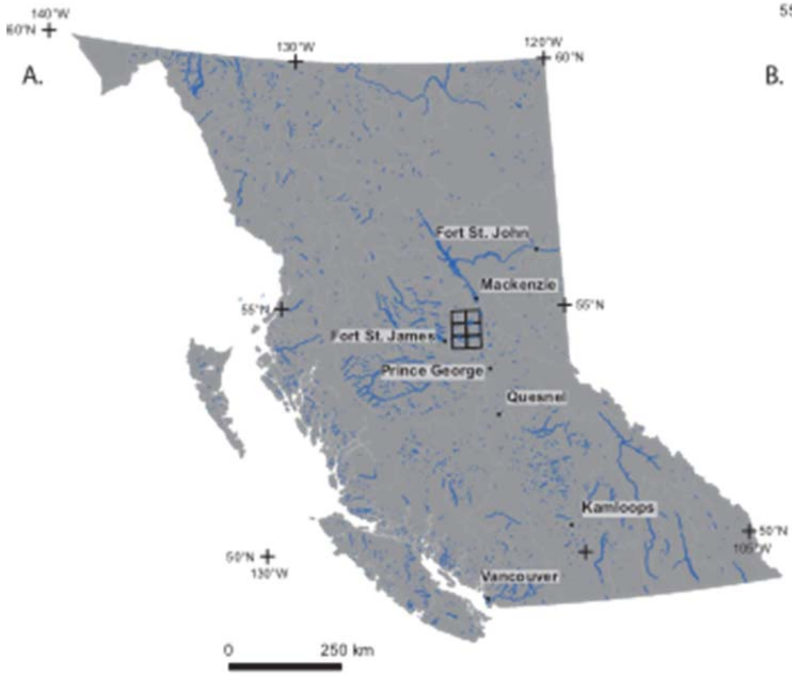

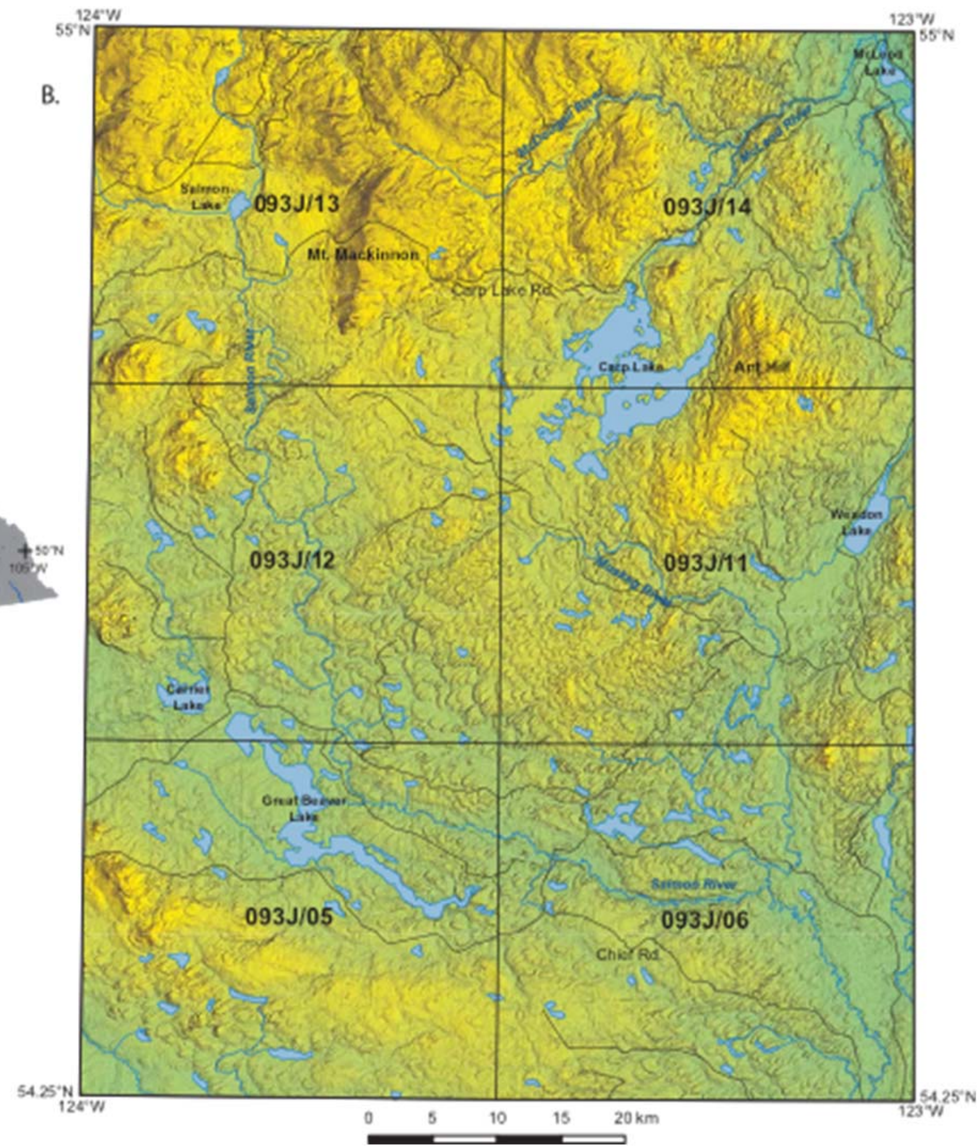

Figure 1: A) Location of study area in relation to communities in the vicinity. B) Shaded elevation model of the 6 1:50,000 map areas that comprise the study area.

LOCATION AND PHYSIOGRAPHY

The study area, located in west-central British Columbia, comprises six, 1:50 000-scale map sheets (NTS 093J/05, 06, 11, 12, 13, and 14; Figure 1). Highway 97, which links Prince George to Fort St. John, runs alongside the east side of the study area and Highway 16, which links Prince George to Fort St. James, runs to the south. A moderately dense network of Forest Service roads provides access to most parts of the study area for fieldwork based out of Prince George, Fort St. James, McLeod Lake and Mackenzie. The majority of the study area lies in the relatively low relief of the Interior Plateau (Holland, 1976; Mathews, 1986), including its subdivisions, the Nechako Plain and the Fraser Basin. These areas are characterized by drumlinized till, glaciofluvial outwash and esker deposits with glaciolacustrine deposits occurring in the southern regions. The northwestern part of the study area occurs within the Nechako Plateau and is characterized by till mantles and exposed bedrock.

BEDROCK GEOLOGY

The study area straddles four of the terranes that make up the Canadian Cordillera (Cache Creek, Slide Mountain, Quesnel, Kootenay) while the most northeastern corner of it extends into the Rocky Mountain Assemblage (Figure 2). A complex assemblage of intrusive and extrusive rocks of the Slide Mountain terrane occurs in the east. The Cache Creek terrane is represented by Pennsylvanian and Permian limestone in the southwestern portion of the study area, with basalts occurring just to the south. The Rocky Mountain assemblage in the northeastern corner of the study area comprises Silurian to Devonian sandstone and quartzite. The Quesnel terrane dominates the study area and is composed primarily of Late Triassic to Early Jurassic arc volcanic rocks of the Witch Lake succession and volcaniclastic rocks of the Cottonwood River succession, both part of the Nicola Group (Logan et al., 2010). The Nicola Group was previously referred to as the Takla Group (Struik, 1994), following first usage. It was correlated with Takla Group rocks to the west within the Stikine terrane. The Nicola Group comprises: a) mainly basaltic to dacitic volcaniclastic rocks and subordinate coherent volcanic rocks, each with augite-porphyry textures (particularly characteristic of the Quesnel terrane), which form an eastern facies of alkaline to subalkaline augite-phyric basaltic andesite; b) coeval and partly comagmatic plutons ranging from calcalkaline (in the west) to alkaline (in the east); and c) sedimentary rocks, including shale, limestone and epiclastic deposits.

Stratigraphically overlying these terranes are a series of overlap assemblages ranging from Upper Cretaceous to Miocene sedimentary rocks and Cretaceous to Pliocene volcanic rocks. The latter includes the dominantly Miocene Chilcotin basalts and Eocene felsic volcanic rocks. Intrusive rocks, paragneiss and metasedimentary rocks of the Wolverine metamorphic complex were exposed during Eocene extension. The metamorphism and plutonism occurred in the late Cretaceous and Paleogene, and the protolith for the paragneiss and metasedimentary rocks are likely Precambrian and Early Paleozoic (Struik, 1994). Recent compilation has assigned these rocks to the Kootenay terrane (Logan et al., 2010).

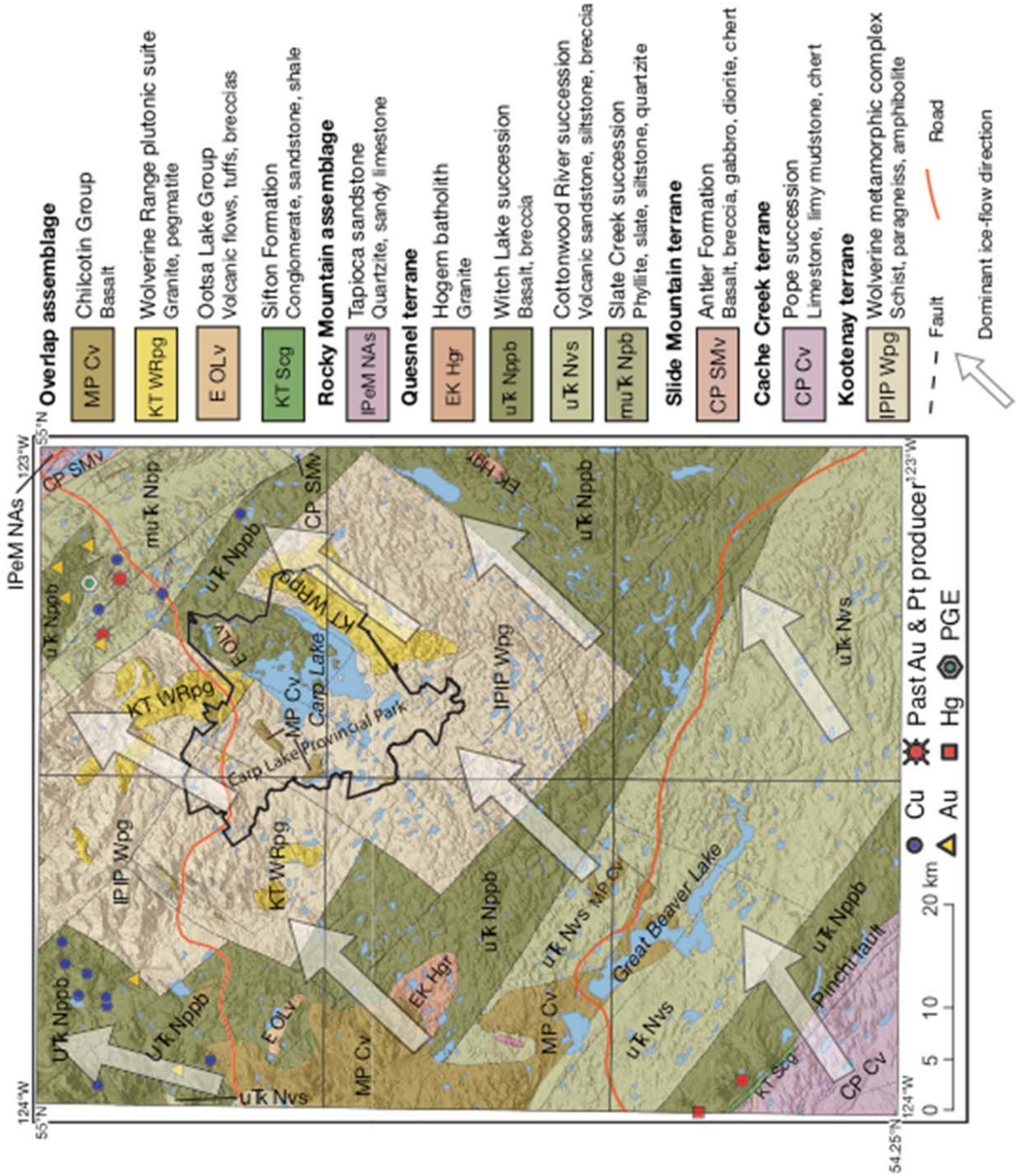

Figure 2: Simplified bedrock geology of the study area. Modified after Logan et al., (2010) and Struik, (1994). Mineral showings reported in MINFILE (BC Geological Survey, 2010) are also indicated.

Mineral Occurrences

Within the study area are twelve Cu showings, six Au showings, one platinum group elements (PGE) showing, two Hg showings and two past-producing Au and Pt deposits (MINFILE; BC Geological Survey, 2010; Figure 2).

The two past producers are the McDougall River and McLeod River placer deposits (MINFILE 093J 007 and 012; BC Geological Survey, 2010). Both deposits occur in the northeastern part of the study area, underlain primarily by the Mississippian Slide Mountain Group. Cariboo Northern Development Co. Ltd. and Northern Reef Gold Mines Ltd. worked the McDougall River placer gold deposit from around 1931 to 1935, with total reported production of approximately 1750 g Au (62 oz). From 1981 to present, the area has received renewed interest, including heavy mineral, soil, silt and rock sampling; geological mapping; airborne very low frequency (VLF) and magnetometer surveys; and ground VLF and magnetometer surveys by a variety of companies. At McDougall River, Au and Pt were extracted from shallow gravel deposits on both banks of the river, with additional clasts retrieved from cracks and crevices in the bedrock. Locally sheared rocks and quartz veins may be the source of the placer Au and PGE. Heavy mineral samples have yielded high Au and Ag contents, and many of the placer Gold grains recovered are angular to wiry, consistent with minimal transport from a local bedrock source. The coincident electromagnetic (EM) and magnetic anomalies could represent the local source for Au.

The two Hg showings (Mount Prince Southeast and Northwest, MINFILE 093J 010, 093J 011) in the southwestern part of the study area are associated with the Pinchi fault. Both showings are characterized by small volumes of cinnabar hosted by carbonate-altered and sheared Nicola Group mafic volcanic rocks, commonly associated with quartz stringers. Most of the other mineral showings in the study area are small with minimal associated exploration activity.

Mount Milligan (MINFILE 093N 194) is a Cu-Au porphyry developed prospect to the northwest of the study area in Quesnel terrane. In this area, Triassic to Lower Jurassic volcanic and subordinate sedimentary rocks of Nicola Group are interpreted to be the extrusive phase of the Hogem intrusive suite. Many Cu-Au mineral showings are associated with the Hogem batholith and smaller coeval intrusions (LeFort et al., 2011). The Nicola Group in the Mount Milligan area is informally subdivided into a lower, predominantly sedimentary Inzana Lake succession, and an upper, predominantly volcaniclastic, Witch Lake succession. The Witch Lake succession hosts the Mount Milligan deposit and is characterized by augite-phyric volcaniclastic and coherent basaltic andesite, with subordinate epiclastic beds. Regional mapping and petrographic studies in the Mount Milligan area indicate that the Witch Lake basaltic andesite and associated sedimentary rocks have been subjected to strong potassic alteration detectable for up to 4 km from the deposit. Witch Lake succession volcanic rocks were intruded by syn- and post-depositional gabbro, diorite, granodiorite, monzonite and syenite (Logan et al., 2010). Recent work has shown that mineralization at Mount Milligan is dominated by an early Cu-rich porphyry stage, with later mineralization characterized by enrichments in Au, PGE, As, Sb, Bi, Te and B (LeFort et al., 2011).

Regional Quaternary Geology

The Cordilleran Ice Sheet has repeatedly covered British Columbia and portions of Yukon, Alaska and Washington over the last two million years (Armstrong et al., 1965; Clague, 1989). At its maximum extent, the Cordilleran Ice Sheet was up to 900 km wide and up to 2000–3000 m thick over the Interior Plateau, closely resembling the present-day Greenland Ice Sheet (Clague, 1989). A more comprehensive history of the Cordilleran Ice Sheet can be found in Jackson and Clague (1991) and Clague and Ward (2011).

The major sources of regional ice that covered central British Columbia advanced from accumulation centres in the Coast, Skeena, Omenica and Cariboo mountains (Tipper, 1971a, b; Levson and Giles, 1997; Plouffe, 1997, 2000, Ward et al, 2009). The study area occurs near the convergence of these three advancing ice fronts, making it difficult to determine which ice centre(s) had the most influence on ice flow direction and dispersal in the early parts of the Late Wisconsinan. Previously reported ice-flow indicators (Tipper, 1971a; Paulen and Bobrowsky, 2003), in combination with data from this study, suggest that it was mainly ice from the Coast Mountains to the west and the Coast and Cariboo mountains to the south that affected the area. Absolute chronological information on the movement and/or confluence of ice fronts through the study area is limited. Although it is known that ice was advancing out of the Coast Mountains by 28.8 ka (GSC-95, Clague, 1989), it is not clear when this advance reached the central Interior Plateau. Ice, possibly sourced from the Cariboo Mountains (Paulen and Bobrowsky, 2003), covered the Bowron Valley sometime after 19.9 ka (AA44045, Ward et al., 2008). According to Bobrowsky and Rutter (1992), ice advancing from the Omineca Mountains into what is now the north arm of Williston Lake occurred sometime after 15 180 ±100 BP (TO-708).

The dominant ice flow in the study area is relatively easy to demonstrate using the orientations of the numerous macro-forms. The macro-forms were initially compiled from existing maps (Tipper 1971) and the resolution was increased with observations made during mapping for this project (Figure 3). The dominant ice flow indicators generally consist of drumlins, flutings, crag and tails, and streamlined bedrock (Figure 3). The interaction of the two sources resulted in a general northeastern transport direction with minor variation across the 6 sheets; the large streamlined forms are approximately ENE in the southwest portion of the study area and curve northward, being NNE in the north of the study area.

Small-scale ice flow indicators were measured in the field such as grooves, striations and rat-tails. These micro-flow indicators were measured at a total of 22 sites (Figure 3). At some of these sites, multiple ice flow directions were recorded, at others only one dominant direction was observed. Finding micro-flow indicators (e.g., striations, rat-tails) was challenging due to the lack of bedrock exposures in parts of the field area, and the weathered nature of some of the out crops present. In most cases, except for some fresh road cuts, micro-flow indicators were only found after sediment, usually till, was scraped, brushed or washed off bedrock surfaces.

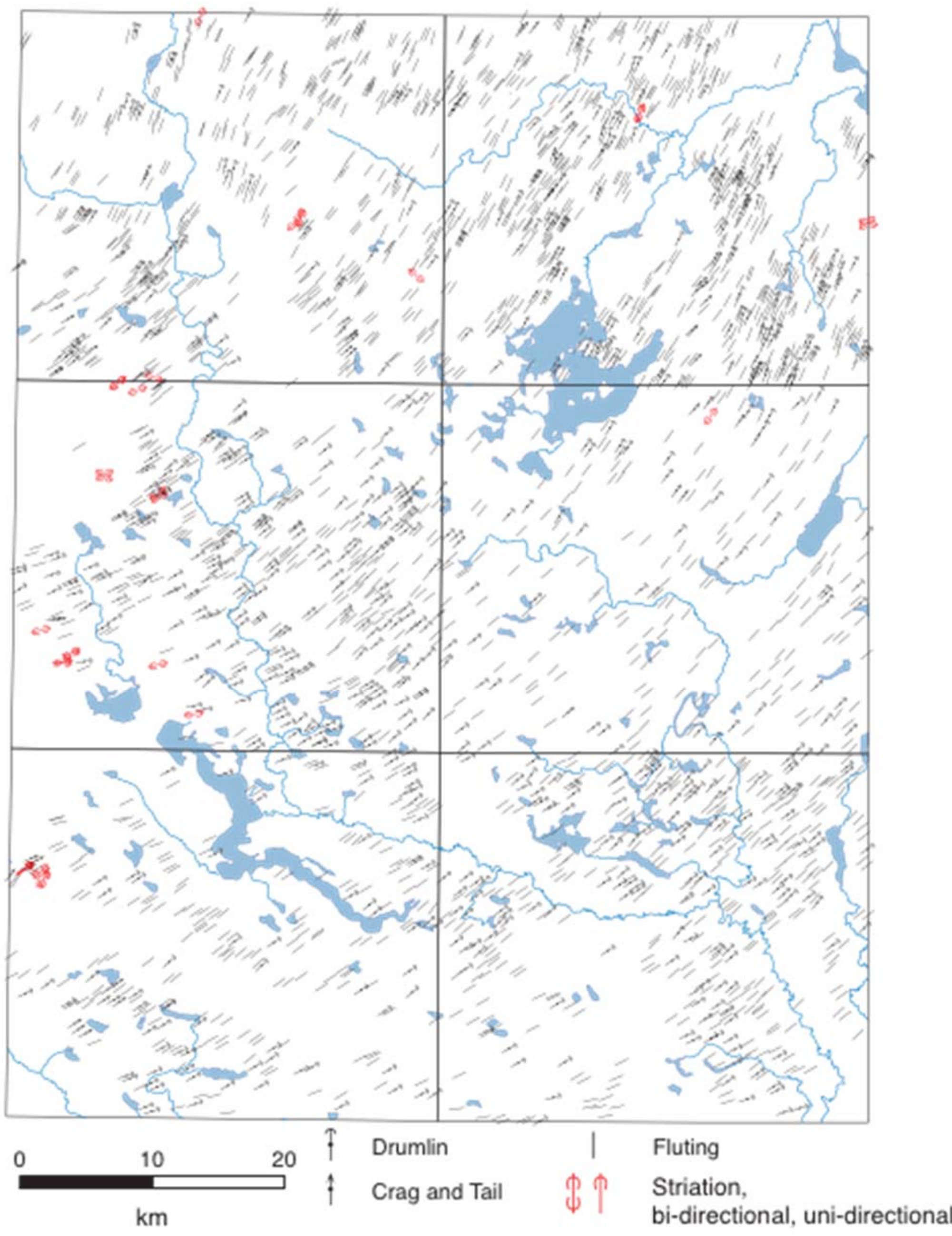

Figure 3: Ice flow for the study area indicated by streamlined landforms, such as drumlins and flutings, and striations.

The orientation of elongate clasts in till were measured at 12 sites. These till fabrics can be used to interpret the genesis of a till unit and the direction of ice flow that deposited it. Fabrics and striations were used to add detail and a relative chronology to the ice flow history that is described in Sacco et al. (2012).

METHODS

Geochemistry

Basal till samples were collected at approximately 760 sites within the study area, during the summers of 2008, 2009, and 2010. There are slightly different numbers of samples for the different size fractions analyzed owing to a small number of lost or mislabeled samples (see Appendices). Basal till in the study area is typically a dense, dark grey, sandy to clayey silt matrix supported diamicton containing 25-40% gravel sized material (clasts). The average sample density is approximately 1 sample per 8 km^2, but there are some zones with no samples and some zones with higher density. In some areas sampling was not possible because of access problems, road deactivation and lack of roads, or lack of suitable sample media, such as areas of eolian, glaciofluvial and glaciolacustrine deposits. In addition, no sampling occurred in Carp Lake Provincial Park.

At each sample site three separate ~900 g samples were collected for: 1) analysis of the clay-size fraction (< 0.002 mm) by inductively coupled plasma mass spectrometry (ICP-MS), following an aqua regia digestion, at Acme Analytical Laboratories Ltd. (Vancouver, BC); 2) analysis of the silt- plus clay-sized fraction (< 0.063 mm) by instrumental neutron activation analysis (INAA) at Activation Laboratories Inc. (Ancaster, ON); and 3) for archive at the Geological Survey of Canada. These archive samples will be available for future analysis for either improved detection limits or different elements.

Clay-sized separations were produced by centrifuge at Acme Analytical Laboratories Ltd. (Vancouver, BC). Typically, between 0.5–0.8 kg of till were processed, which on average yielded approximately 5 g of clay. The clay splits were analyzed by ICP-MS for 36 elements (analytical package 1DX) following leaching in a hot (95°C) aqua-regia digestion (detection limits are listed in the appendixes with the data). Up to 5 g of clay is analyzed to overcome potential nugget effects for Au.

The silt plus clay-sized fraction (<0.063 mm) of till samples (on average, 24 g of material was used) were analyzed for 35 elements by INAA (analytical package 1D, enhanced option)(detection limits are listed in the appendixes with the data). Hoffman (1992) describes the analytical procedure as follows. An aliquot and an internal standard (one for every eleven samples) are irradiated with flux wires at a thermal neutron flux of $7 \times 10^{12} \cdot n \cdot cm^{-2} \cdot s^{-1}$. After a seven-day decay, the samples are counted on a high purity Ge detector. Using the flux wires, the decay-corrected activities are compared to a standard calibration curve. The standard included is only a check on accuracy and is not used for calibration purposes. From 10–30% of the samples are rechecked by re-measurement.

Heavy Minerals

Bulk till samples (> 10 kg) were collected at every 4 – 5 sites sampled for geochemical analysis. In total, 152 samples were collected. Heavy mineral concentrates (HMCs) were separated at Overburden Drilling Management Limited (Nepean, ON) and were panned for gold grains, platinum group metals (PGM) and uraninite. Bulk samples were disaggregated, followed by separation of the > 2mm and < 2 mm fractions. The < 2mm fraction was then preconcentrated on a shaking table, with the finest, heaviest fraction being panned. Gold, uraninite, and platinum group elements (PGEs) were then examined under optical microscope to provide grain counts as well as grain morphology. More detailed descriptions of the methods are provided in Averill (2001). Sulfide and cinnabar grain counts were also made, although where n > 20, these counts are estimates.

The table concentrate was then sieved and the < 0.25 mm fraction subsequently separated using heavy liquid at 3.2 g/cm^3. This < 0.25 mm fraction was then analyzed by INAA at Becquerel Laboratories (Mississauga, ON) using their BQ-NAA-1 package (with the addition of Hg for 2009 and 2010 samples). The concentrate is placed in vials, which are stacked into one-foot (30 cm) long bundles for irradiation at the McMaster Nuclear Reactor, which has flux of 8 x $10^{12} \cdot n \cdot cm^{-2} \cdot s^{-1}$. After a typical decay period of six days, the irradiated samples are loaded onto a high resolution, coaxial germanium detector that constructs a spectrum of gamma-ray energies versus intensities. The counting time is twenty to thirty minutes per sample. Quantitative elemental contents are derived by comparison of peak positions and area with library standards. For the 2009 and 2010 samples, several elements, such as Hg, Ni, Zr, Rb, Au, had variable and higher than usual detection limits because of elevated Cr, REE and Th contents (Steve Simpson, pers. comm., 2011). For example, Au usually has a detection limit of 2 ppb but here it ranges from 5 to 42 ppb depending on the sample. However, the samples taken in 2008 did not have this issue.

QUALITY CONTROL

Discriminating geochemical trends caused by geological features from variation due to spurious sampling or analytical error is critical for assessing the reliability of regional geochemical survey data. A combination of field duplicates, analytical duplicates and reference standards are used to estimate the accuracy and precision of these analytical data. Every 20 sample group submitted for commercial analysis contain a field duplicate, an analytical duplicate (split and inserted into the sample sequence at the lab after preparation), and a reference standard (either an in-house BC Geological Survey standard or a certified Canada Centre for Mineral and Energy Technology [CANMET] standard). No field or analytical duplicates were done for the heavy mineral samples, owing to the large sample sizes required.

Scatter-plots of the analytical and duplicate pairs were generated and a selection is shown in Figure 4 and 5, with the rest of the analysis in Appendix 1. Precision for the aqua regia (clay fraction) ICP-MS analyses is typically much better than for the INAA (silt+clay) analyses. For the ICP-MS analyses, correlation coefficients for the field duplicates are typically higher than those for the analytical duplicates and are generally above + 0.9. More than 80 percent of the total variation among the duplicates is accounted for by the Field Duplicate 1 – Field Duplicate 2 correlation. Correlation coefficients for the INAA duplicates are generally much lower, with better precision for Co, Cr, Th and the REE than the other analytes. The higher precision for the ICP-MS data is in part related to lower detection limits and less variation in grain size, but also likely reflects better instrument capabilities.

Four CANMET till standards (TILL 1, 2, 3 and 4), BC Geological Survey sediment (RD 29) and till standards (SM, Till 99), and two quartz blank samples were analysed with the survey samples to measure analytical accuracy and precision. All of the standards data is compiled in Appendix 1. The INAA quartz blank sample results reveal amounts of As, Br, Co, Cr, La, Ce, Th and Sc in the 1 to 10 ppm range and less than 0.2 % Fe. Trace amounts (< than 1 ppm) of Cu, Pb, Co, Mn, Sr and Ba in the blanks are detectable by the aqua regia digestion-ICP-ES analysis. Element concentrations detected in the blank samples may reflect traces in the quartz and not necessarily sample contamination during the analysis.

Precision is below +/- 8 % RSD for As, Cd, Co, Cr, Cu, Hg, Mn, Mo, Ni, Pb, Sb, V and Zn in standards analysed by aqua regia ICP-MS and below +/- 8% RSD for As, Br, Co, Cr, Fe, La, Ce, Th and Sc in GSB Till 99. Accuracy can be accessed from the near-total INAA analyses and measured amounts for most elements are within 5% of the recommended value. Precision and accuracy for elements at different concentration is best shown by the CANMET standards data (Appendix 1). The INAA analyses of CANMET. Gold shows considerable variation although the mean and recommended values are very similar. The large measured Ba differences compared to the recommended value are difficult to explain. Table 2 lists precision and CANMET recommended values (hot aqua regia analyses) for CANMET Till 1, 2, 3 and 4. Gold precision (%RSD) for three of the standards is below +/- 30% and most other elements have a precision below +/- 8% RSD. Lower precision (i.e. above 8%) commonly reflects a low element concentrations measured in the standard.

RESULTS

Elements with the most significance to potential economic mineralization in the project area are discussed below. Note that we analyzed different size fractions by different analytical methods. In some cases, commodity elements are not analyzed by both methods (e.g., Cu was not determined by INAA). Furthermore, depending on where an element is sequestered in a sample, comparisons between size fractions may have greater or lesser utility, as discussed below. Note also that aqua regia digestion is not total, silicate and resistant oxides are not digested to any great extent. By contrast, INAA is a total method. Thus, the differences between results for the clay-size versus the silt plus clay-size fractions are not only a function of analytical method (partial versus total), but also a function of where an analyte resides within a

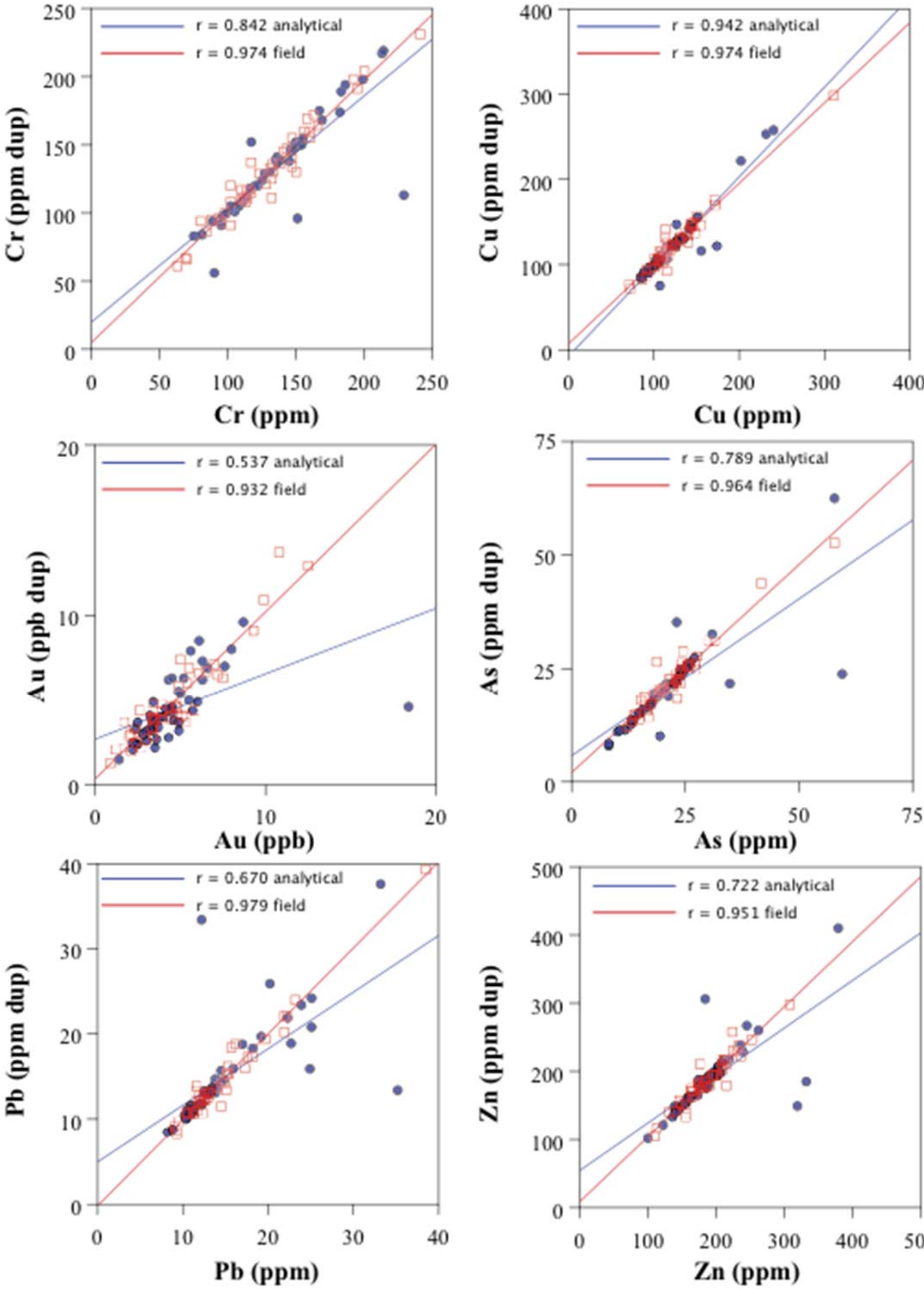

Figure 4: Scatterplots of field and analytical duplicates for selected elements from ICP-MS data from ACME Labs. Scatter plots for all elements are listed in Appendix 1.

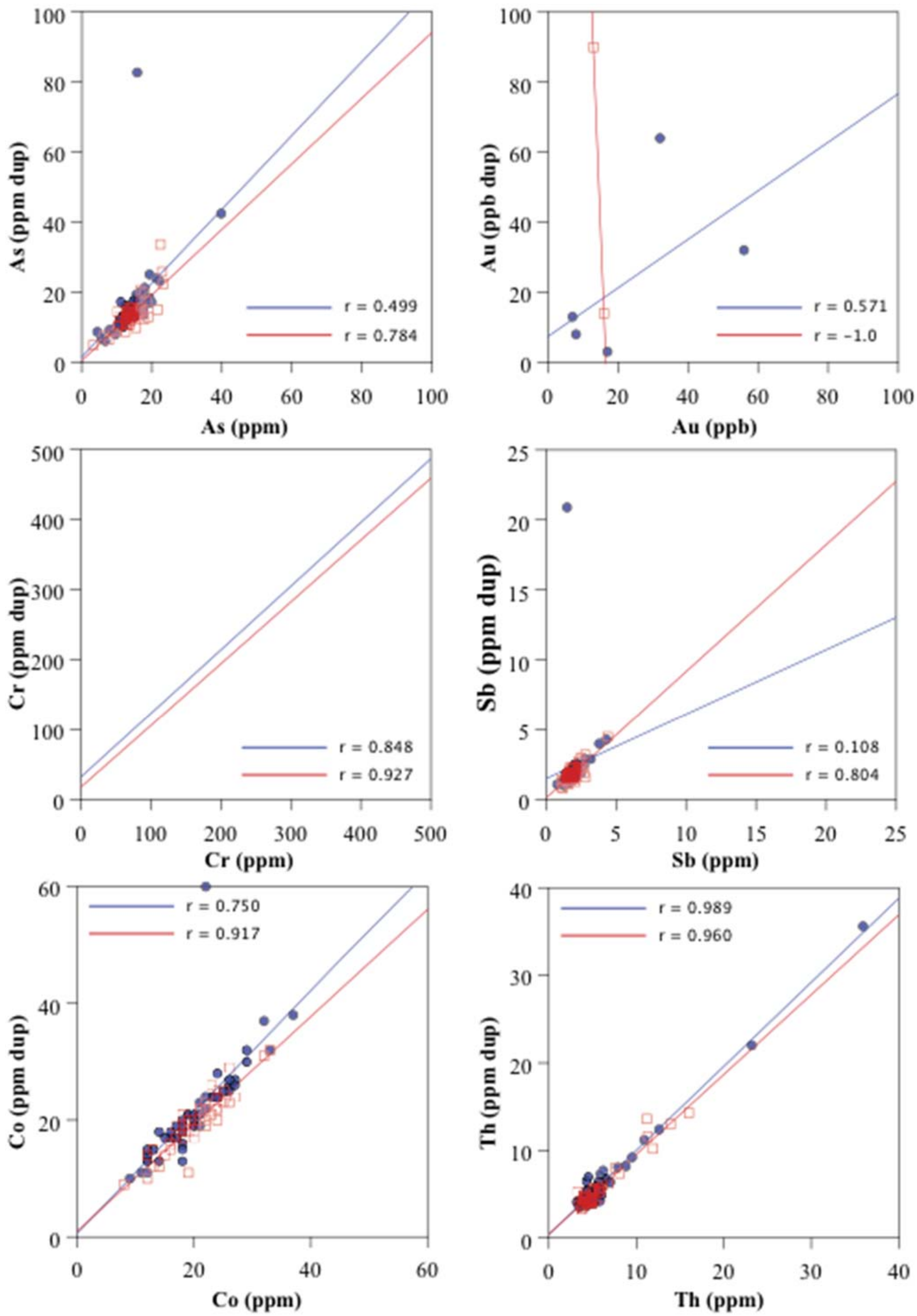

Figure 5: Scatterplots of field and analytical duplicates for selected elements from INAA data from Activation Labs. Scatter plots for all elements are listed in Appendix 1.

sample. For example, As shows good correlations for both field and laboratory duplicates for both size fractions, because As is primarily associated with adsorption to clay-size mineral surfaces (Figure 4). By contrast, Au is more prone to the nugget effect in the silt plus clay-size fraction than Au in the clay fraction (Figure 5).

Till geochemical data (ICP-MS and INAA analysis) is in appendix 2. Heavy mineral data (Grain counts, INAA analysis on the heavy mineral fraction) is in Appendix 3.

Average values are presented below along with one standard deviation and sample count. Sample counts are variable as results below detection are not included in the statistical calculations. Threshold values (percentile) are set based on inflexion points on the cumulative frequency plots (Figure 6); we have not defined a set background value owing to the variability in the geochemical landscape. Where correlations are stated (r values), these represent Pearson Product Moment correlations, statistically significant at least at the 95% confidence interval. In some cases, we also employed R-mode factor analysis, a statistical method to investigate inter-relationships between analytes in a correlation matrix.

Au, As, Ag and Hg in Till

Gold contents in the clay fraction range from less than detection (0.5 ppb) to 294 ppb (average = 5.1 ± 11 ppb, n = 704). Gold contents in the clay fraction show highly anomalous values around the 98th percentile (10 ppb), although there is also a subtle change in slope around the 90th percentile, or 8 ppb (Figure 6a). In the silt plus clay-size fraction, Au contents range from below detection (2 ppb) up to 635 ppb. For the silt plus clay-size fraction, anomalous Au contents occur above the 80th percentile (~8 ppb; Figure 6a); most samples below this threshold were below the detection limit by this method (2 ppb). Anomalous Au contents occur in the northeastern and northwestern parts of the map area for both size fractions (Figures 7a, b), largely coincident with known Au showings. There are also anomalous Au contents, in particular in the silt plus clay-size fraction, to the south, and to a lesser extent, to the east of Carp Lake. There are no known Au showings here. For the clay fraction Au shows the best correlation with Cu (r=0.410). The highest Au content by both methods occurs in the same sample (Figures 7a and 7b) indicating that this anomalous value is not the result of the nugget effect, consistent with this also being the sample with the highest As contents by both methods (Figures 7c and 7d).

All till samples processed for heavy minerals (n = 152) contain visible gold (Figure 8a). Not surprisingly, the distribution of Au by INAA on the heavy mineral concentrates mimics the gold grain distribution (Figure 8b) along with the silt+clay fraction analyzed by INAA (Figure 7b). For the INAA analyses of the HMCs, gold ranges from below detection (5 to 42 ppb depending on the sample) to 2,630 ppb. Gold contents show clearly anomalous values around the 95th percentile (~750 ppb), although there is also a subtle change in slope around the 80th percentile (~ 400 ppb).

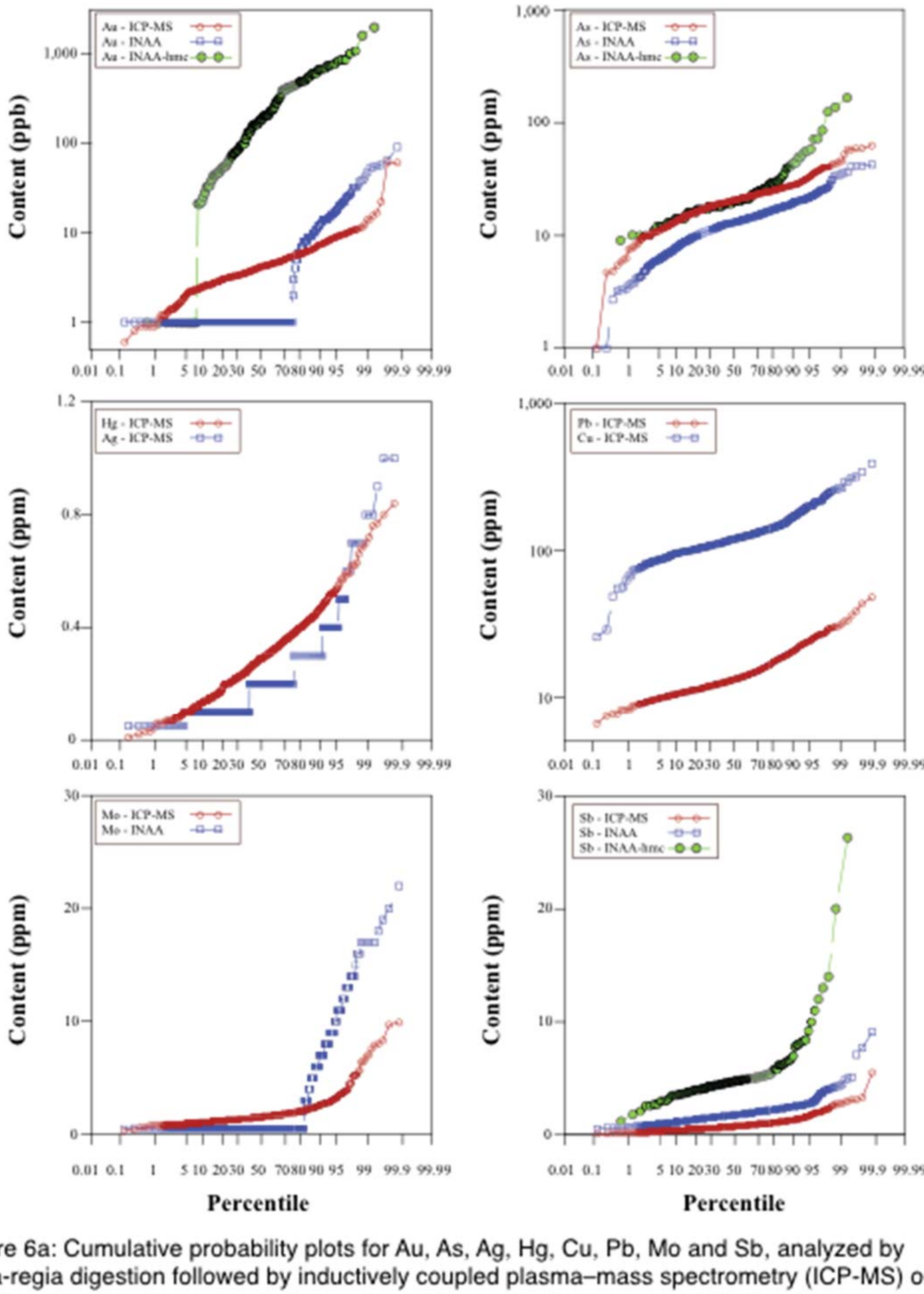

Figure 6a: Cumulative probability plots for Au, As, Ag, Hg, Cu, Pb, Mo and Sb, analyzed by aqua-regia digestion followed by inductively coupled plasma–mass spectrometry (ICP-MS) on the clay-sized fraction and/or instrumental neutron activation analysis (INAA) on the clay plus silt–sized fraction and/or the <.25mm heavy mineral fraction. Anomalous metal concentrations range from 70 to 95th percentiles, where there is a change in slope on the probability plot.

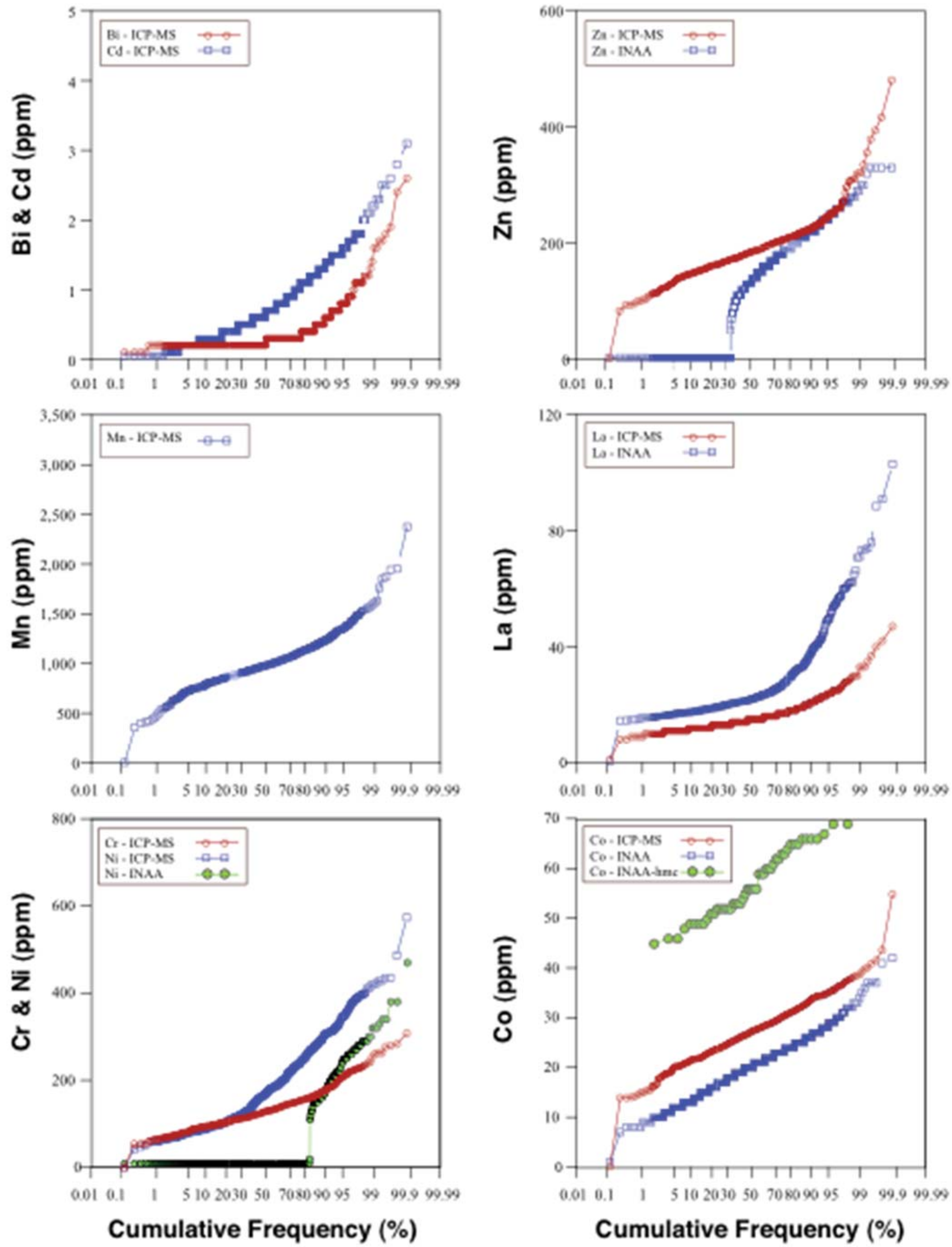

Figure 6b: Cumulative probability plots for Bi, Cd, Zn, Mn, La, Cr, Ni, and Co, analyzed by aqua-regia digestion followed by inductively coupled plasma–mass spectrometry (ICP-MS) on the clay-sized fraction and/or instrumental neutron activation analysis (INAA) on the clay plus silt–sized fraction and/or the <.25mm heavy mineral fraction. Anomalous metal concentrations range from 70 to 95th percentiles, where there is a change in slope on the probability plot.

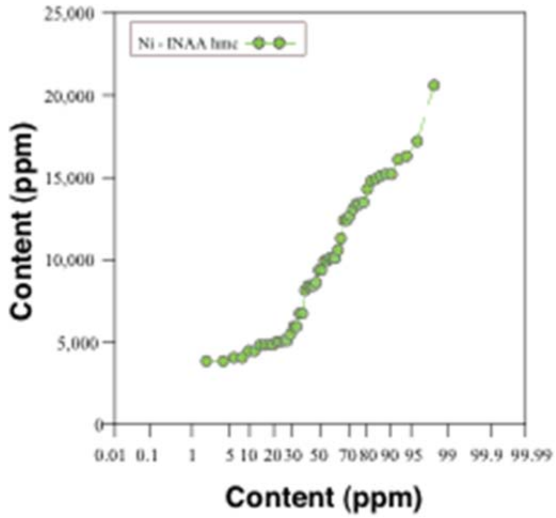

Figure 6c: Cumulative probability plots for Ni analyzed by instrumental neutron activation analysis (INAA) on the <.25mm heavy mineral fraction. Anomalous metal concentrations are approximately at the 95th percentile, where there is a change in slope on the probability plot.

Arsenic is typically considered a pathfinder element for Au. In this study, threshold As contents in till are 32 and 26 ppm, at the 95th and 98th percentiles for the clay and silt plus clay-size fractions, respectively (Figure 6a). Arsenic contents are anomalous in both the northeastern and northwestern sections of the study area (Figures 7c, d), largely coincident with Au anomalies. However, As contents do not appear to be anomalous south of Carp Lake; in contrast, there are anomalous As contents in the west-central part of the study area, primarily in the silt plus clay-size fraction. Au and As show a moderate positive correlation (r=0.372) for the clay fraction based on the R-mode factor analysis, statistically significant at the 99.9% confidence interval. By contrast, the statistical correlation between As and Au for the silt plus clay-size fraction is poor (r=0.112), despite the evident spatial association (Figures 7b, d).

Figure 7 (Next 18 pages): Proportional dot maps of selected elements from till geochemical analyses, central British Columbia: ***a)*** *Au contents (clay-sized fraction) by inductively coupled plasma–mass spectrometry (ICP-MS);* ***b)*** *Au contents (clay plus silt–sized fraction) by instrumental neutron activation analysis (INAA);* ***c)*** *As contents (clay-sized fraction) by ICP-MS;* ***d)*** *As contents (clay plus silt–sized fraction) by INAA;* ***e)*** *Ag contents (clay-sized fraction) by ICP-MS;* ***f)*** *Hg contents (clay-sized fraction) by ICP-MS;* ***g)*** *Cu contents (clay-sized fraction) by ICP-MS;* ***h)*** *Mo contents (clay-sized fraction) by ICP-MS;* ***i)*** *Sb contents (clay-sized fraction) by ICP-MS;* ***j)*** *Pb contents (clay-sized fraction) by ICP-MS;* ***k)*** *Bi contents (clay-sized fraction) by ICP-MS;* ***l)*** *Zn contents (clay-sized fraction) by ICP-MS;* ***m)*** *Cd contents (clay-sized fraction) by ICP-MS;* ***n)*** *La contents (clay plus silt–sized fraction) by INAA;* ***o)*** *La contents (clay-sized fraction) by ICP-MS;* ***p)*** *Cr contents (clay-sized fraction) by ICP-MS;* ***q)*** *Sb contents (silt+clay sized fraction) by INAA;* ***r)*** *Th contents (silt+clay sized fraction) by INAA. Size of dots are proportional to the content with Au-ICP and Au-INAA being represented by log plots. Data are overlaid on the bedrock geology map presented in Figure 2.*

Figure 7a

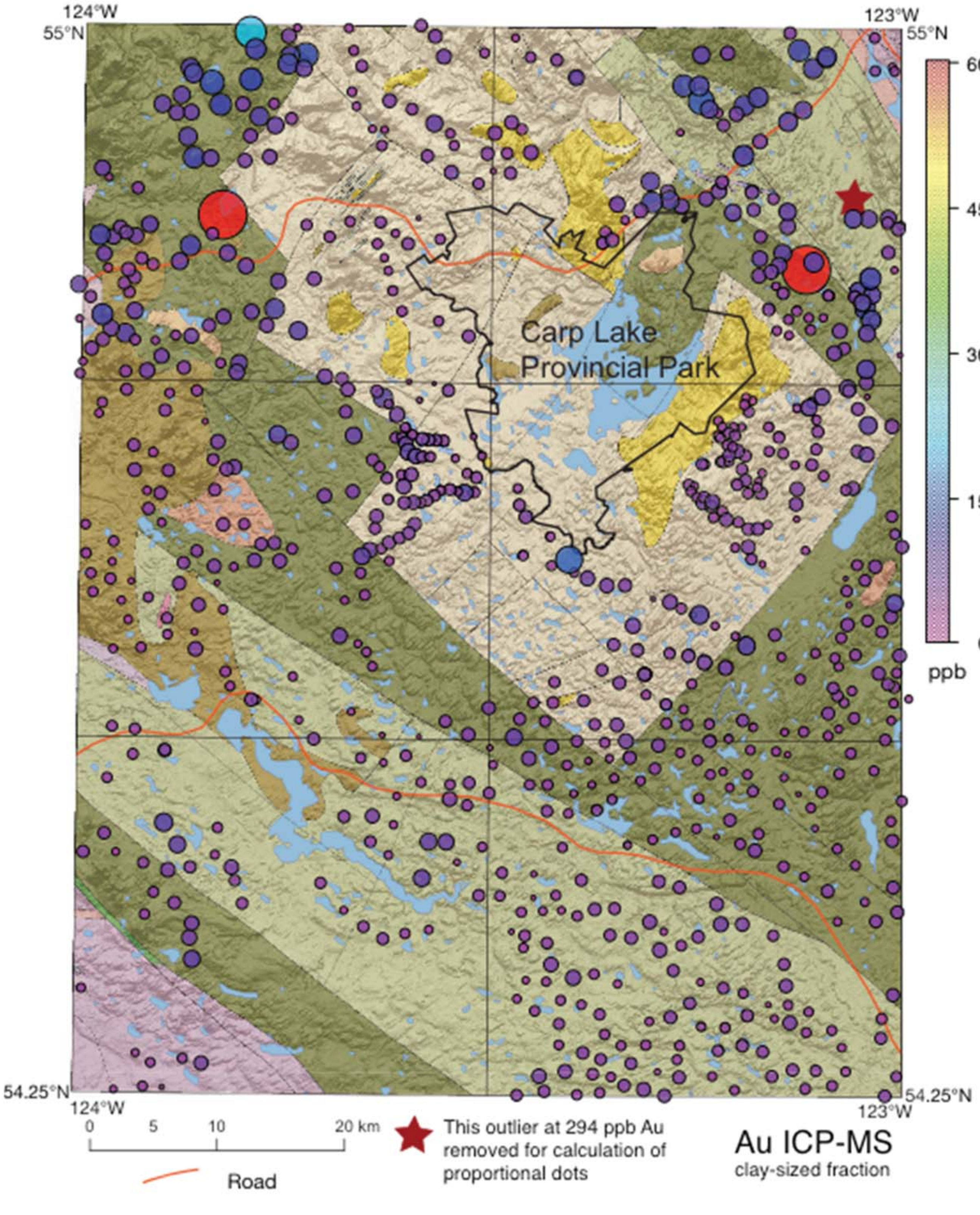
124°W
55°N
123°W
55°N
60.2
45.3
30.4
15.5
0.6
ppb
Carp Lake
Provincial Park
54.25°N
124°W
54.25°N
123°W
0 5 10 20 km
Road
This outlier at 294 ppb Au removed for calculation of proportional dots
Au ICP-MS
clay-sized fraction

Figure 7b

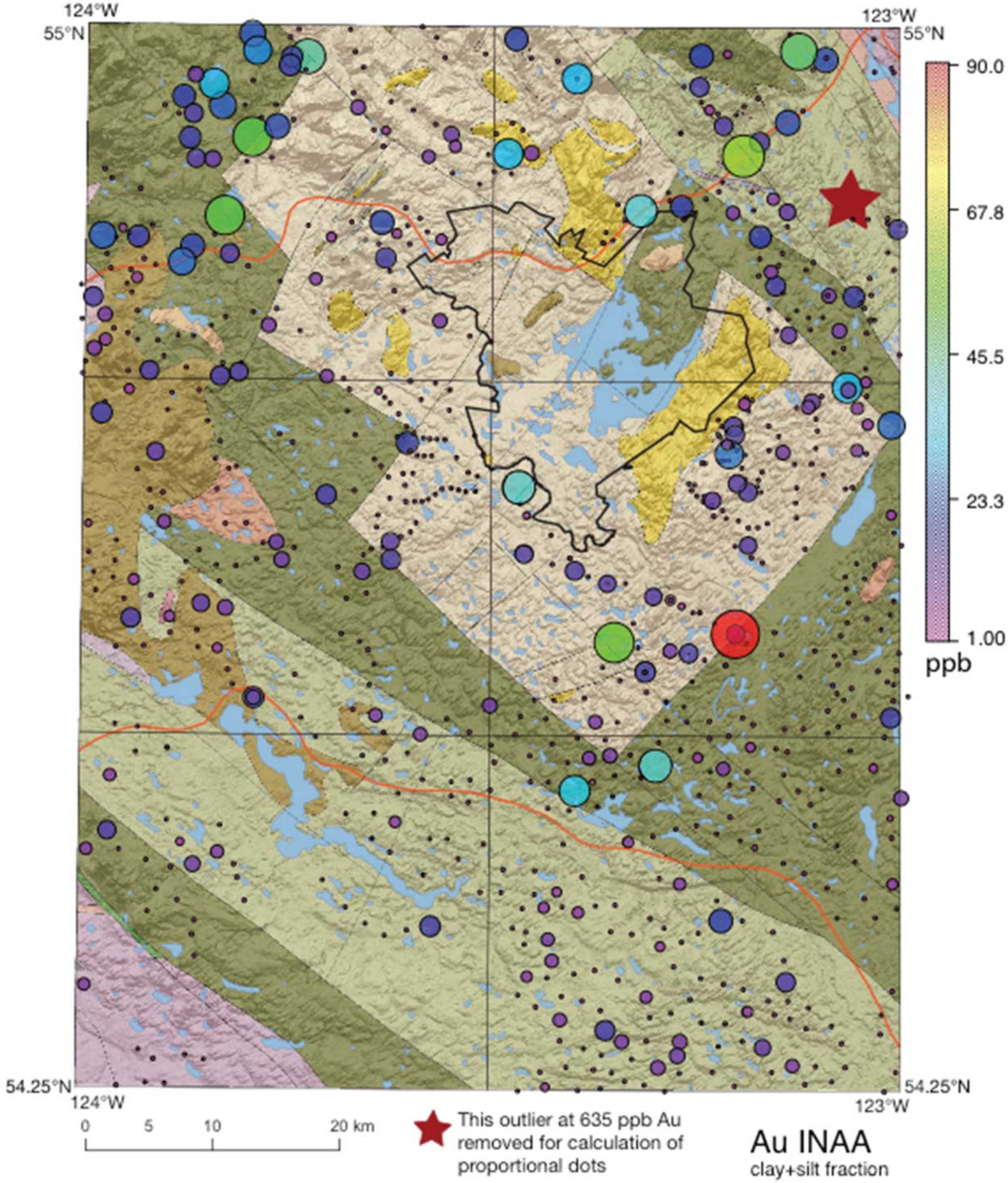

124°W
55°N
123°W
55°N
90.0
67.8
45.5
23.3
1.00
ppb
54.25°N
124°W
123°W
54.25°N
0
5
10
20 km
This outlier at 635 ppb Au removed for calculation of proportional dots
Au INAA
clay+silt fraction

Figure 7c

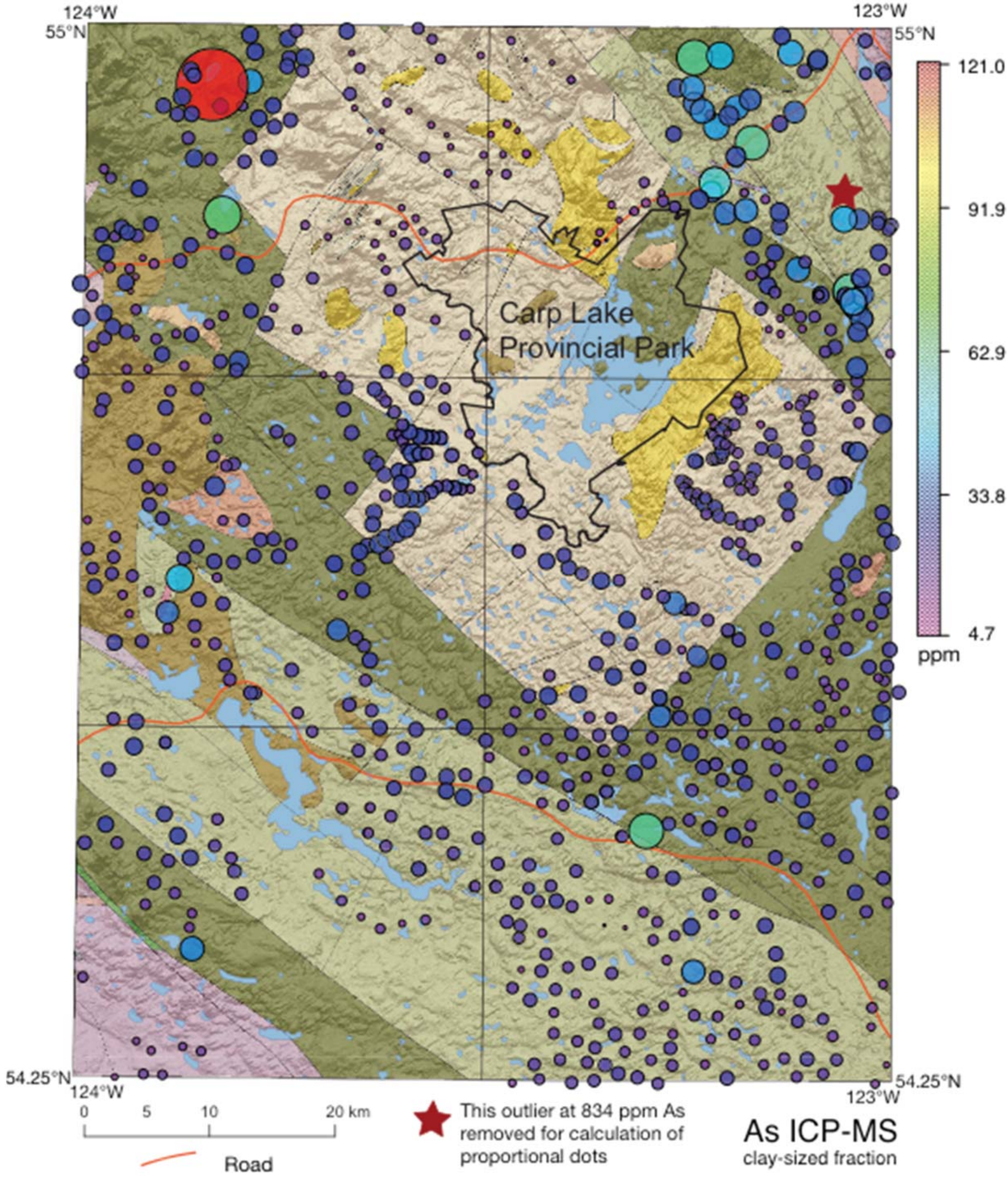

124°W
55°N
123°W
55°N
121.0
91.9
62.9
33.8
4.7
ppm
Carp Lake
Provincial Park
54.25°N
124°W
54.25°N
123°W
0
5
10
20 km
Road
This outlier at 834 ppm As removed for calculation of proportional dots
As ICP-MS
clay-sized fraction

Figure 7d

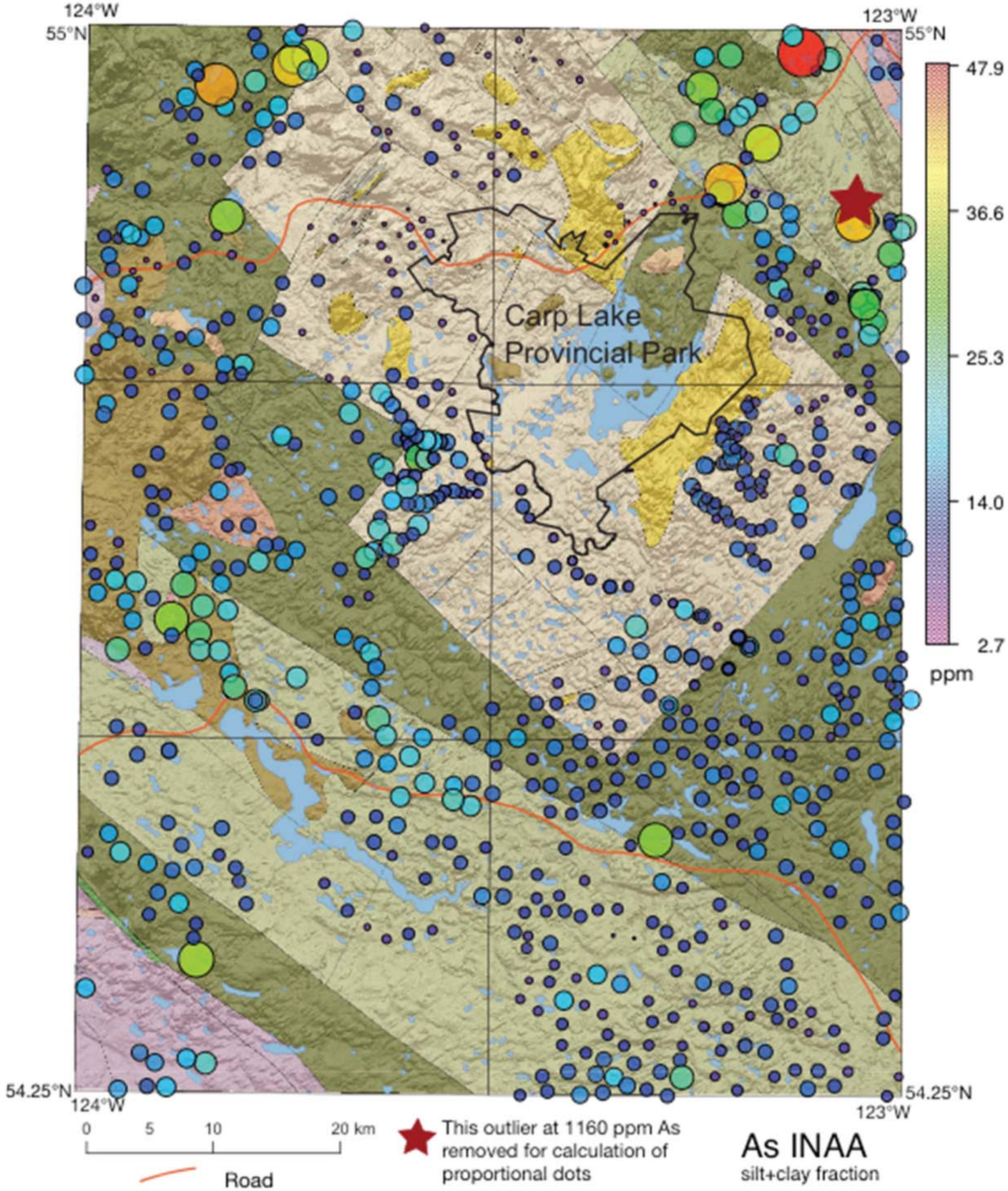

124°W
55°N
123°W
55°N
Carp Lake
Provincial Park
47.9
36.6
25.3
14.0
2.7
ppm
54.25°N
124°W
123°W
54.25°N
0
5
10
20 km
This outlier at 1160 ppm As removed for calculation of proportional dots
Road
As INAA
silt+clay fraction

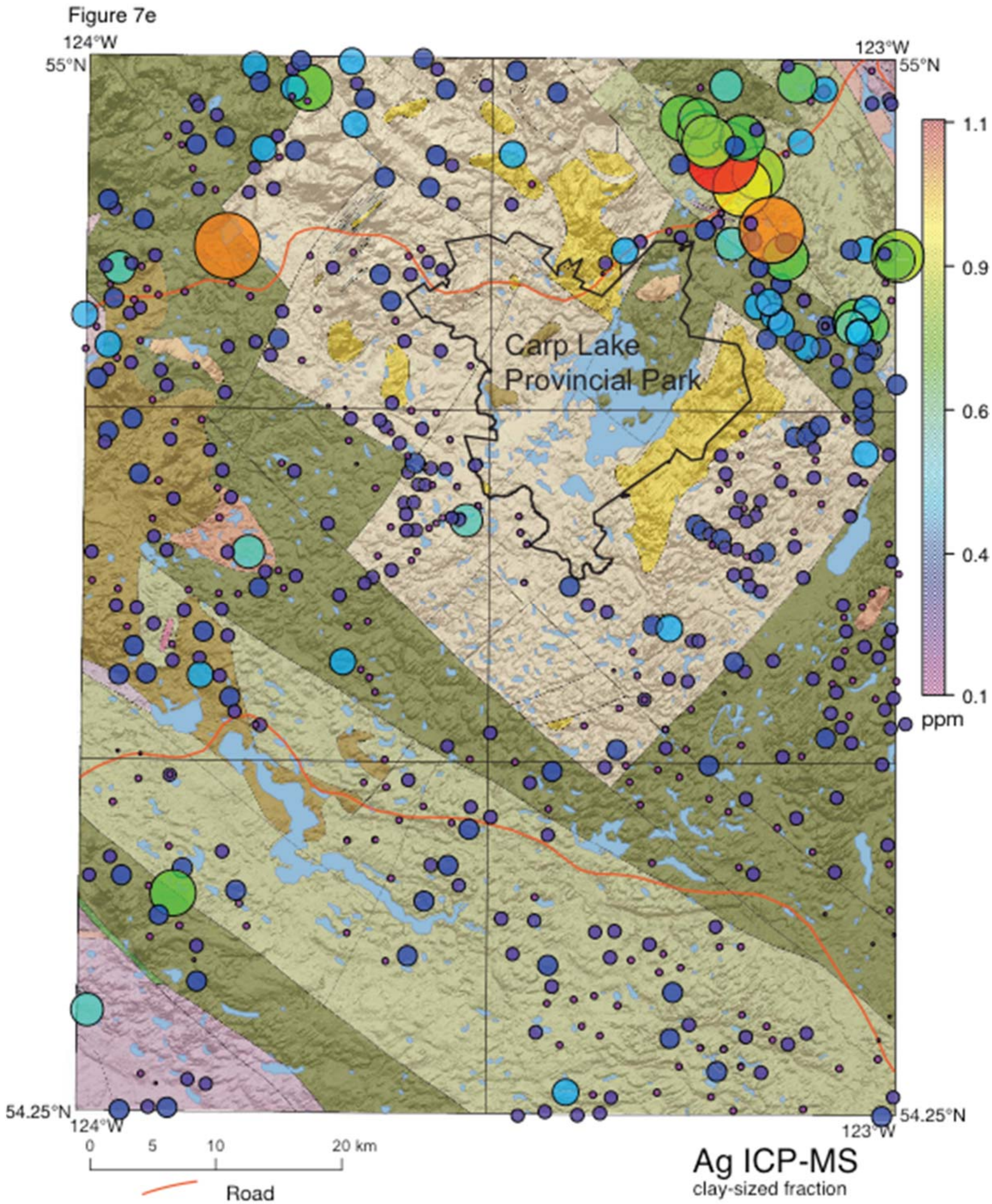

Figure 7e
124°W
55°N
123°W
55°N
Carp Lake
Provincial Park
1.1
0.9
0.6
0.4
0.1
ppm
54.25°N
124°W
123°W
54.25°N
0
5
10
20 km
Road
Ag ICP-MS
clay-sized fraction

Figure 7f

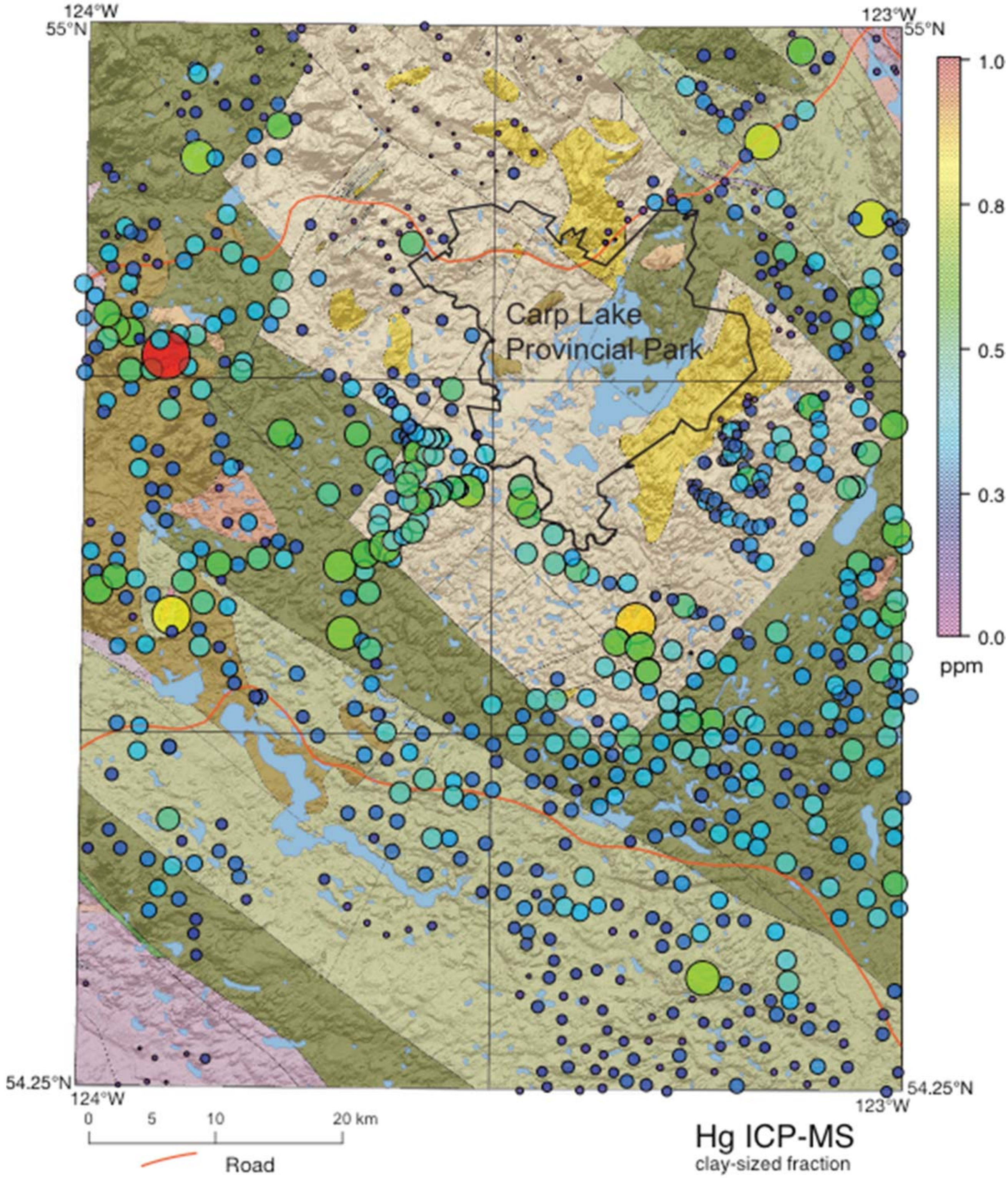

124°W
55°N
123°W
55°N
Carp Lake
Provincial Park
1.0
0.8
0.5
0.3
0.0
ppm
54.25°N
124°W
54.25°N
123°W
0
5
10
20 km
Road
Hg ICP-MS
clay-sized fraction

Figure 7g

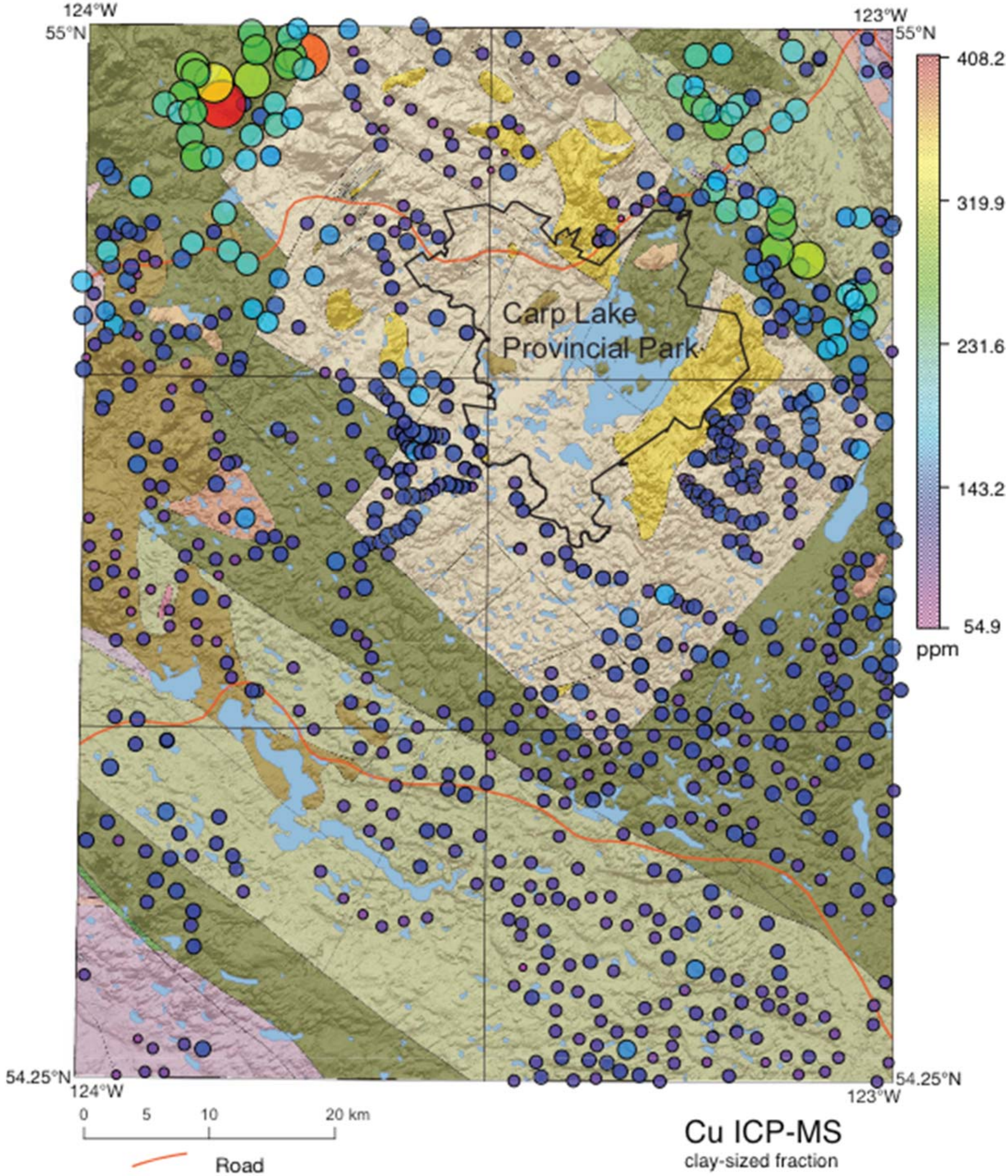

124°W
55°N
123°W
55°N
Carp Lake
Provincial Park
408.2
319.9
231.6
143.2
54.9
ppm
54.25°N
124°W
54.25°N
123°W
0
5
10
20 km
Road
Cu ICP-MS
clay-sized fraction

Figure 7h

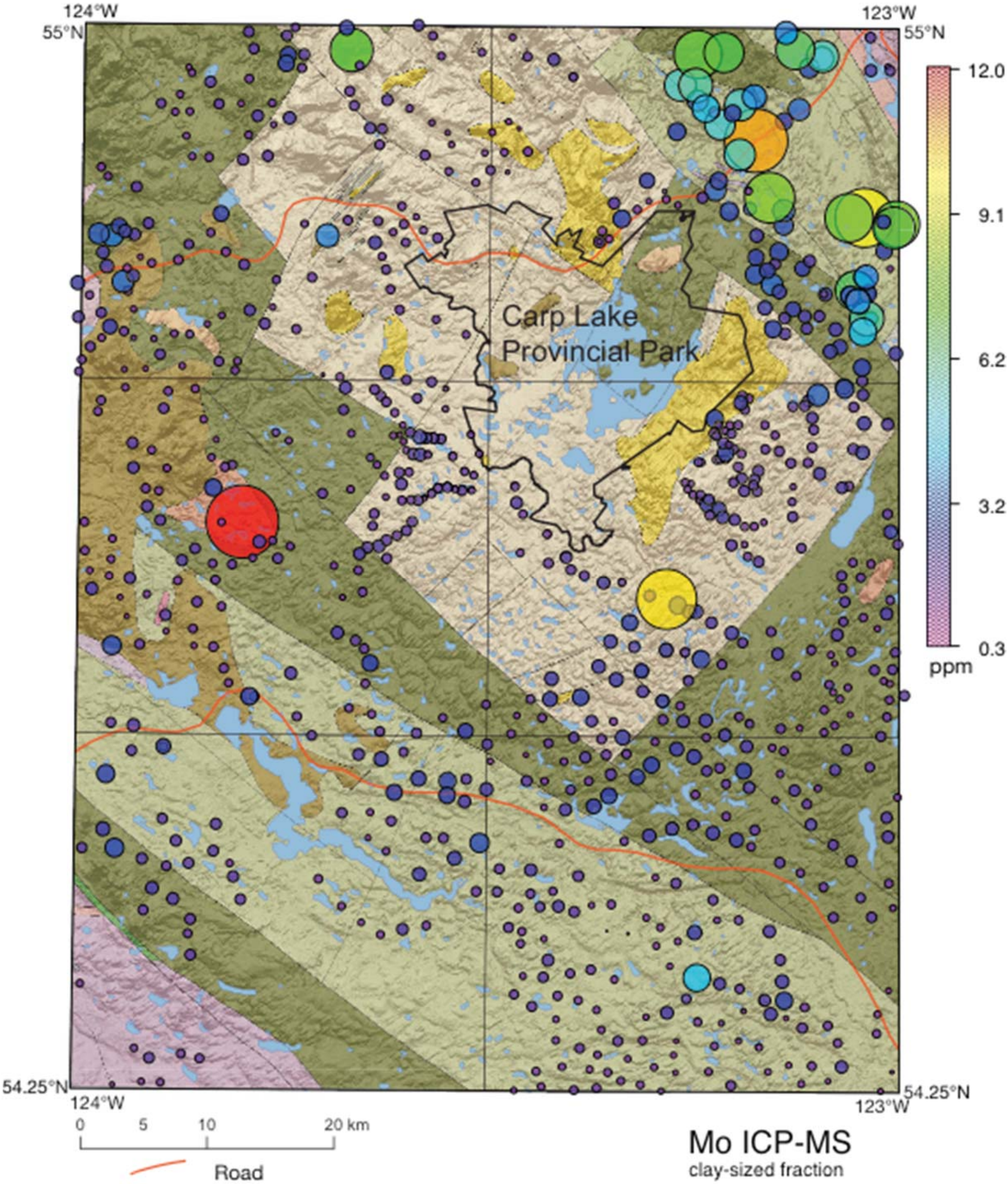

124°W
55°N
123°W
55°N
Carp Lake
Provincial Park
12.0
9.1
6.2
3.2
0.3
ppm
54.25°N
124°W
123°W
54.25°N
0
5
10
20 km
Road
Mo ICP-MS
clay-sized fraction

Figure 7i

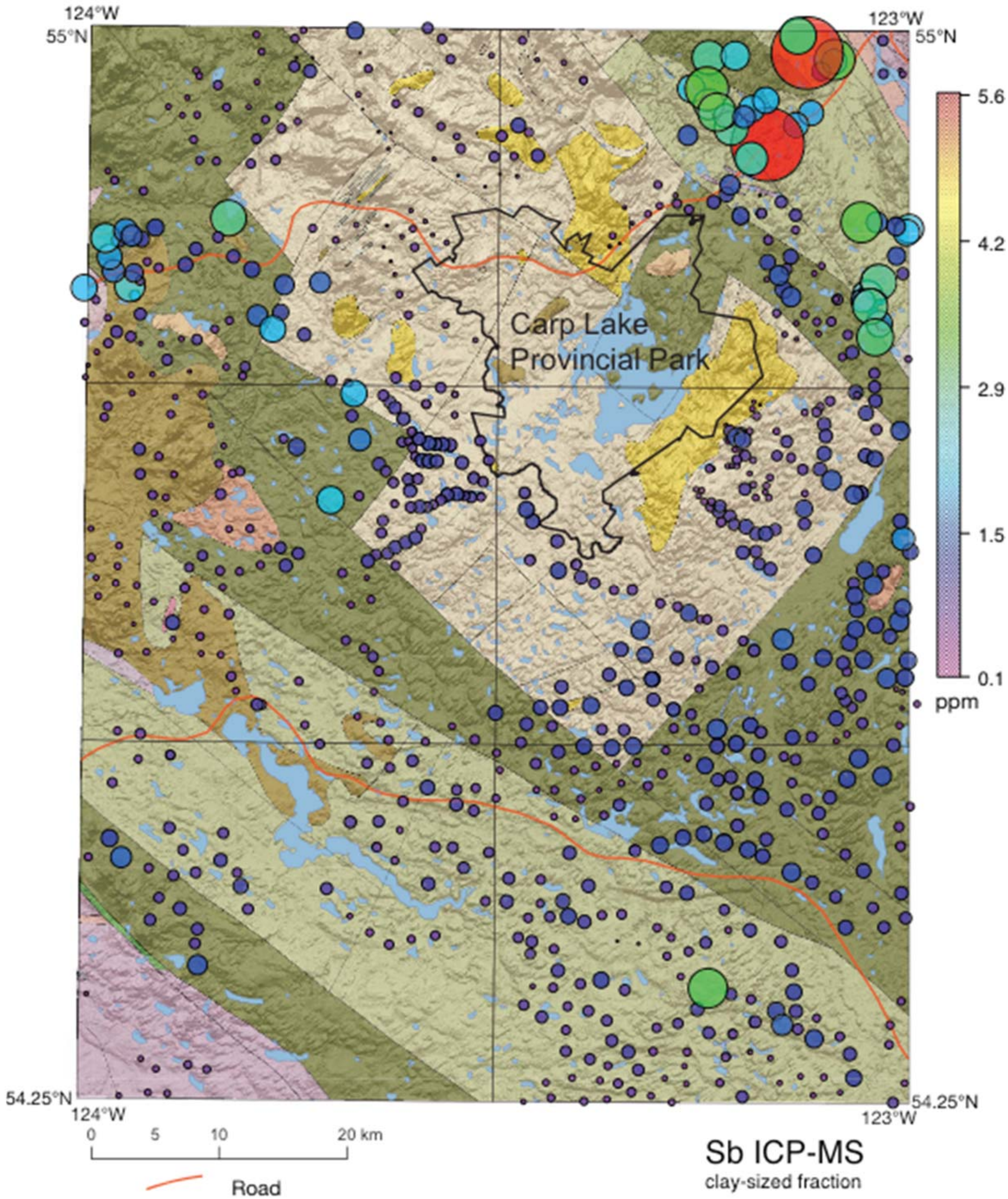

124°W
55°N
123°W
55°N
Carp Lake
Provincial Park
5.6
4.2
2.9
1.5
0.1
ppm
54.25°N
124°W
54.25°N
123°W
0
5
10
20 km
Road
Sb ICP-MS
clay-sized fraction

Figure 7j

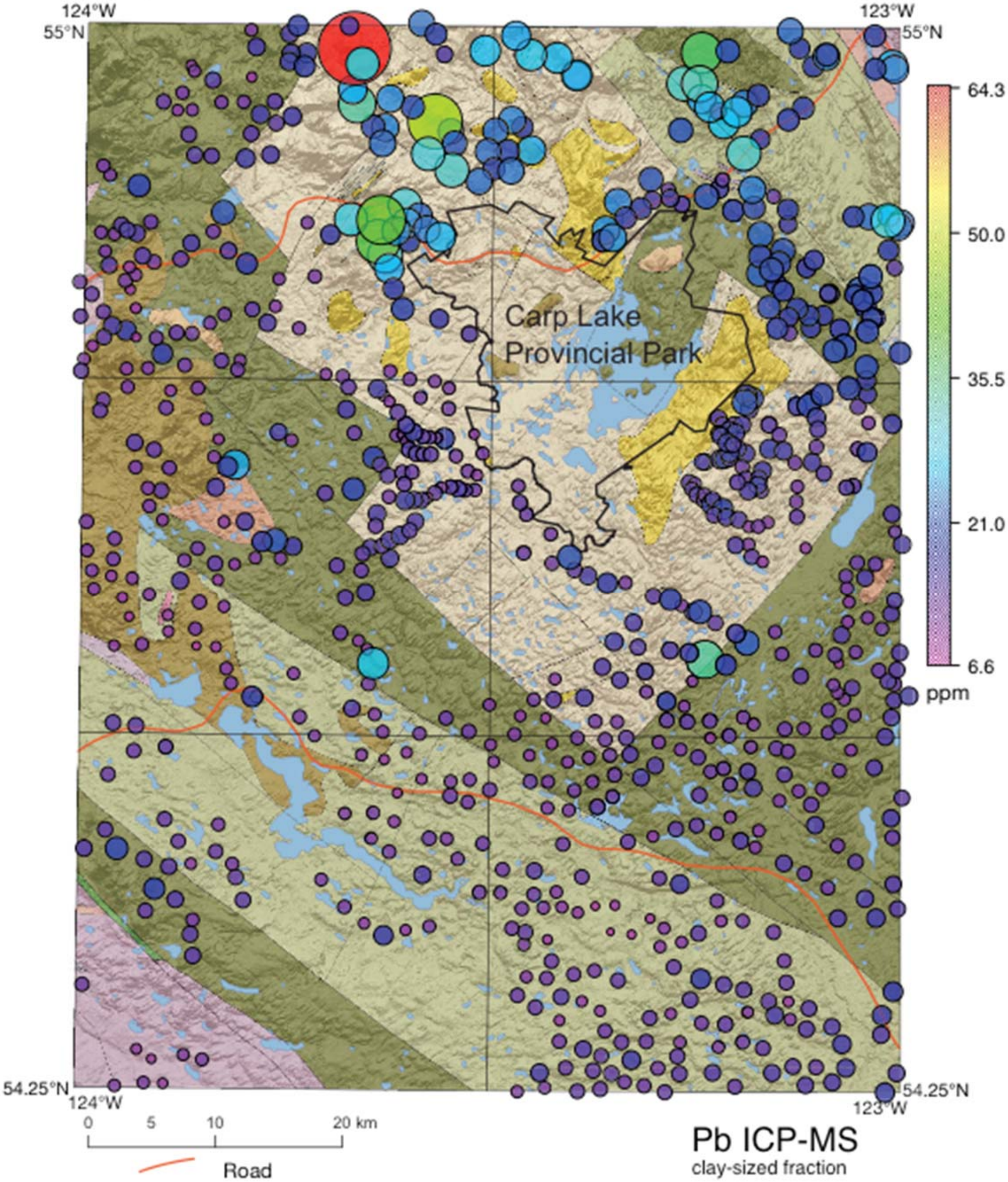

124°W
55°N
123°W
55°N
Carp Lake
Provincial Park
64.3
50.0
35.5
21.0
6.6
ppm
54.25°N
124°W
123°W
54.25°N
0
5
10
20 km
Road
Pb ICP-MS
clay-sized fraction

Figure 7k

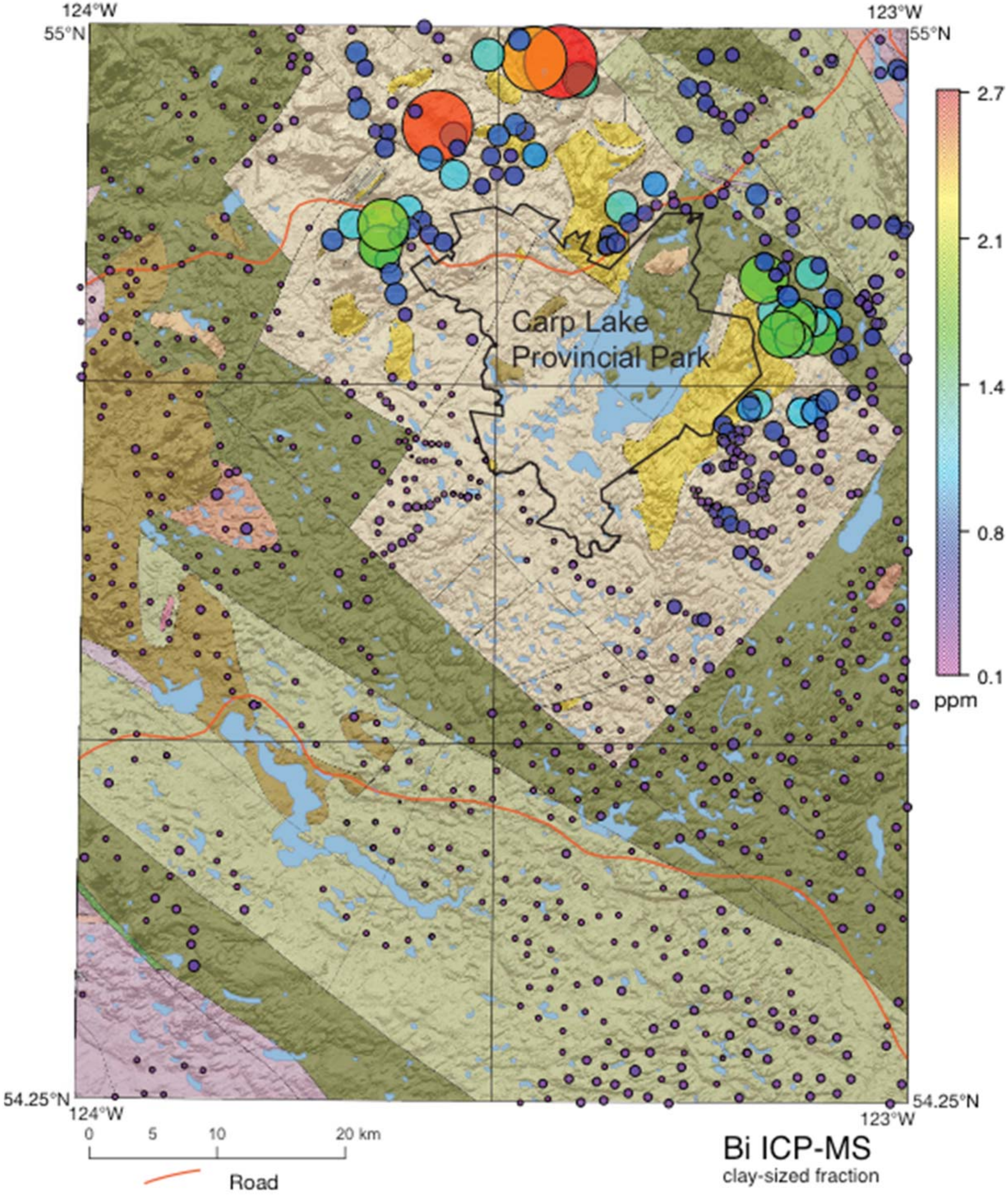
124°W
123°W
55°N
55°N
Carp Lake
Provincial Park
2.7
2.1
1.4
0.8
0.1
ppm
54.25°N
124°W
54.25°N
123°W
0
5
10
20 km
Road
Bi ICP-MS
clay-sized fraction

Figure 7l

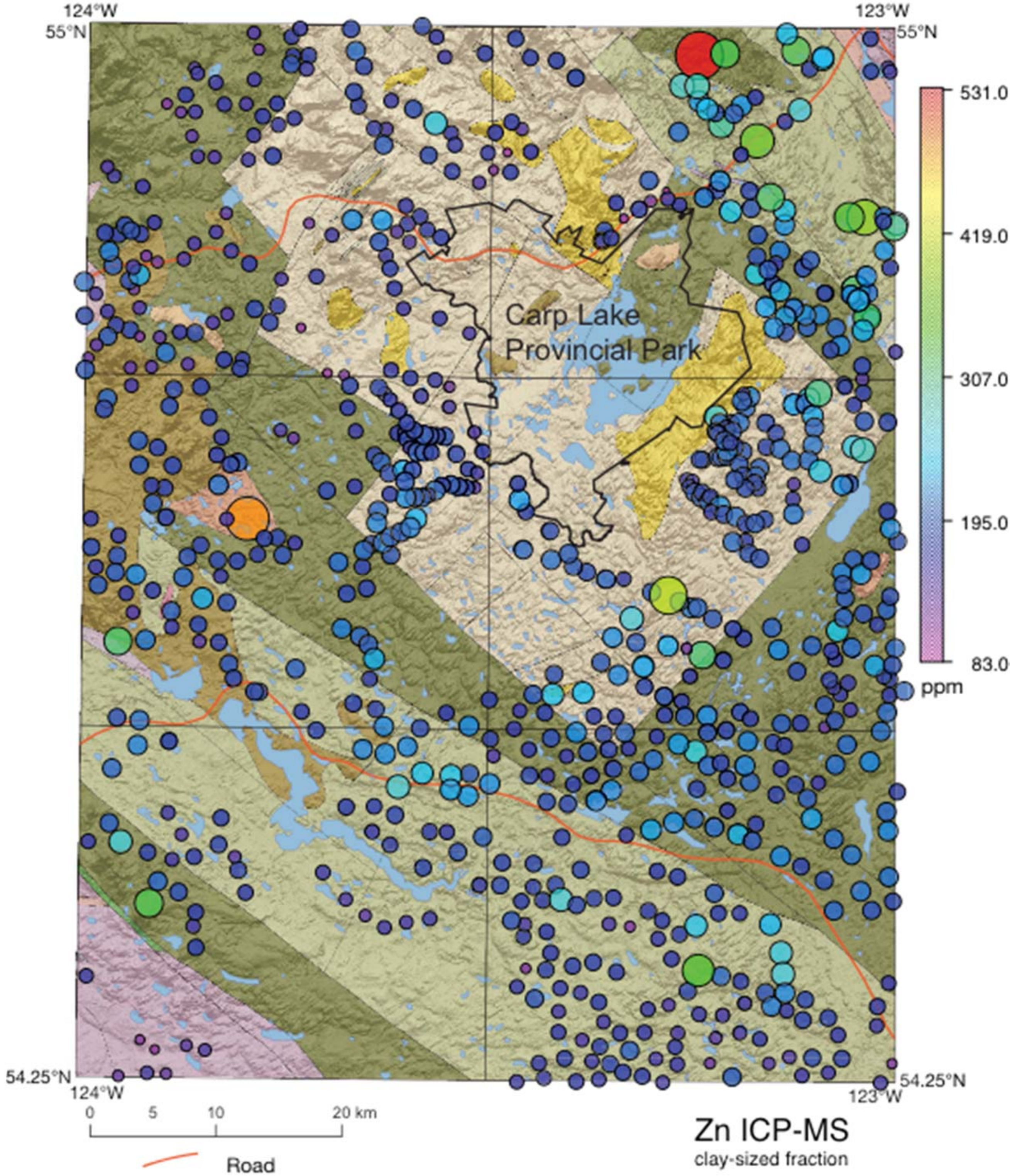
124°W
123°W
55°N
55°N
Carp Lake
Provincial Park
531.0
419.0
307.0
195.0
83.0
ppm
54.25°N
124°W
54.25°N
123°W
0
5
10
20 km
Road
Zn ICP-MS
clay-sized fraction

Geoscience BC

Figure 7m

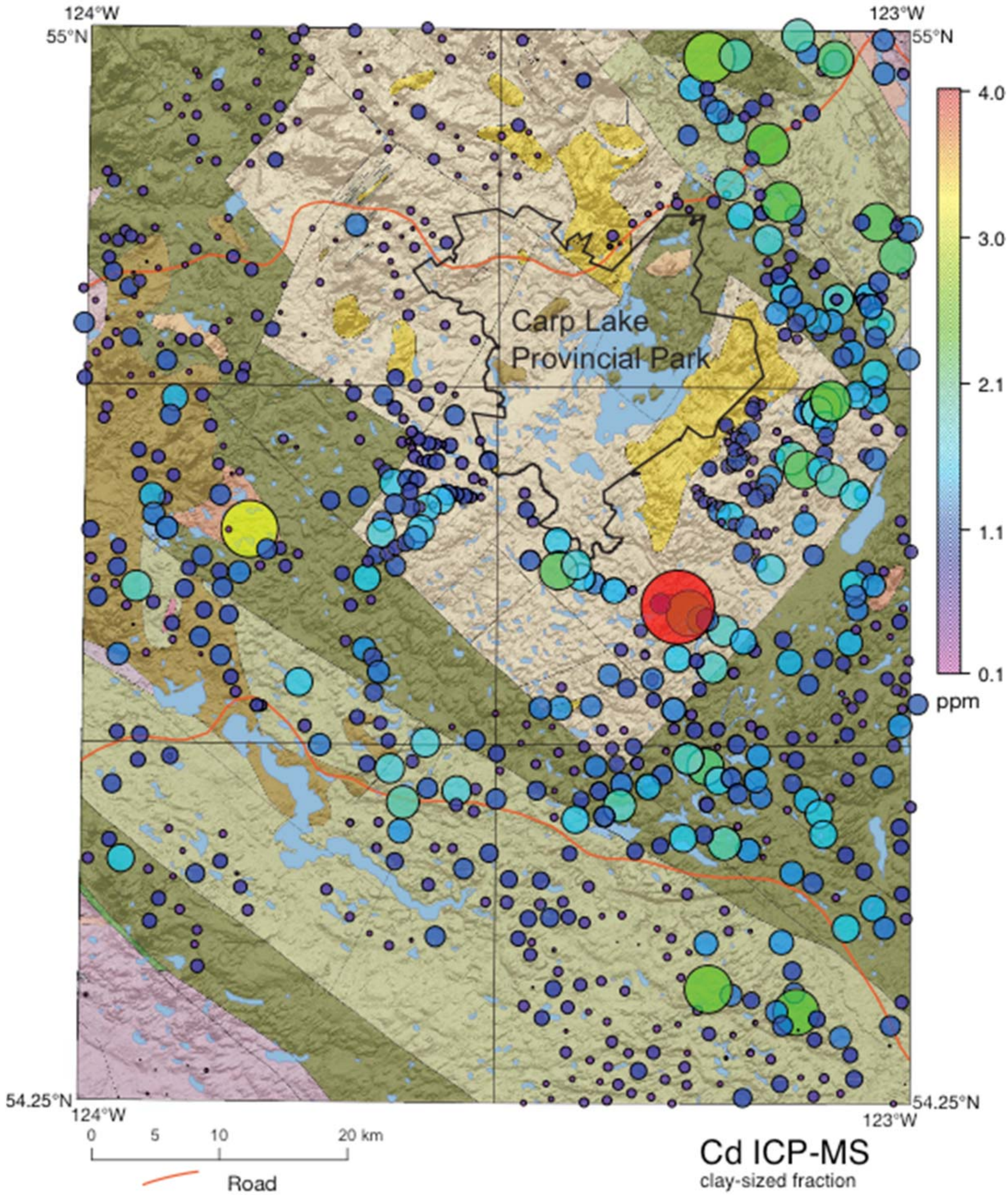

Figure 7n

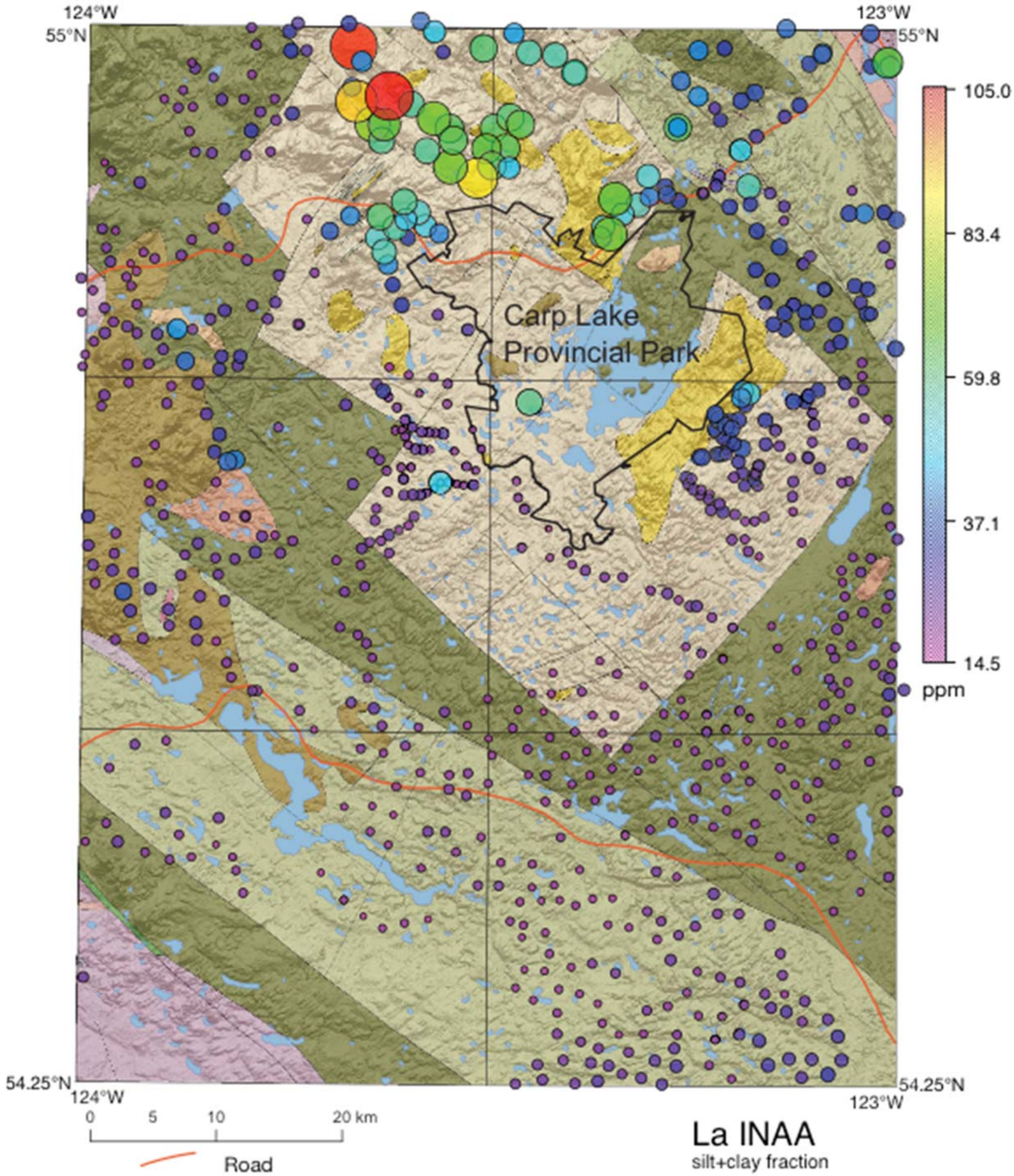
124°W
123°W
55°N
55°N
Carp Lake
Provincial Park
105.0
83.4
59.8
37.1
14.5
ppm
54.25°N
124°W
54.25°N
123°W
0
5
10
20 km
Road
La INAA
silt+clay fraction

Figure 7o

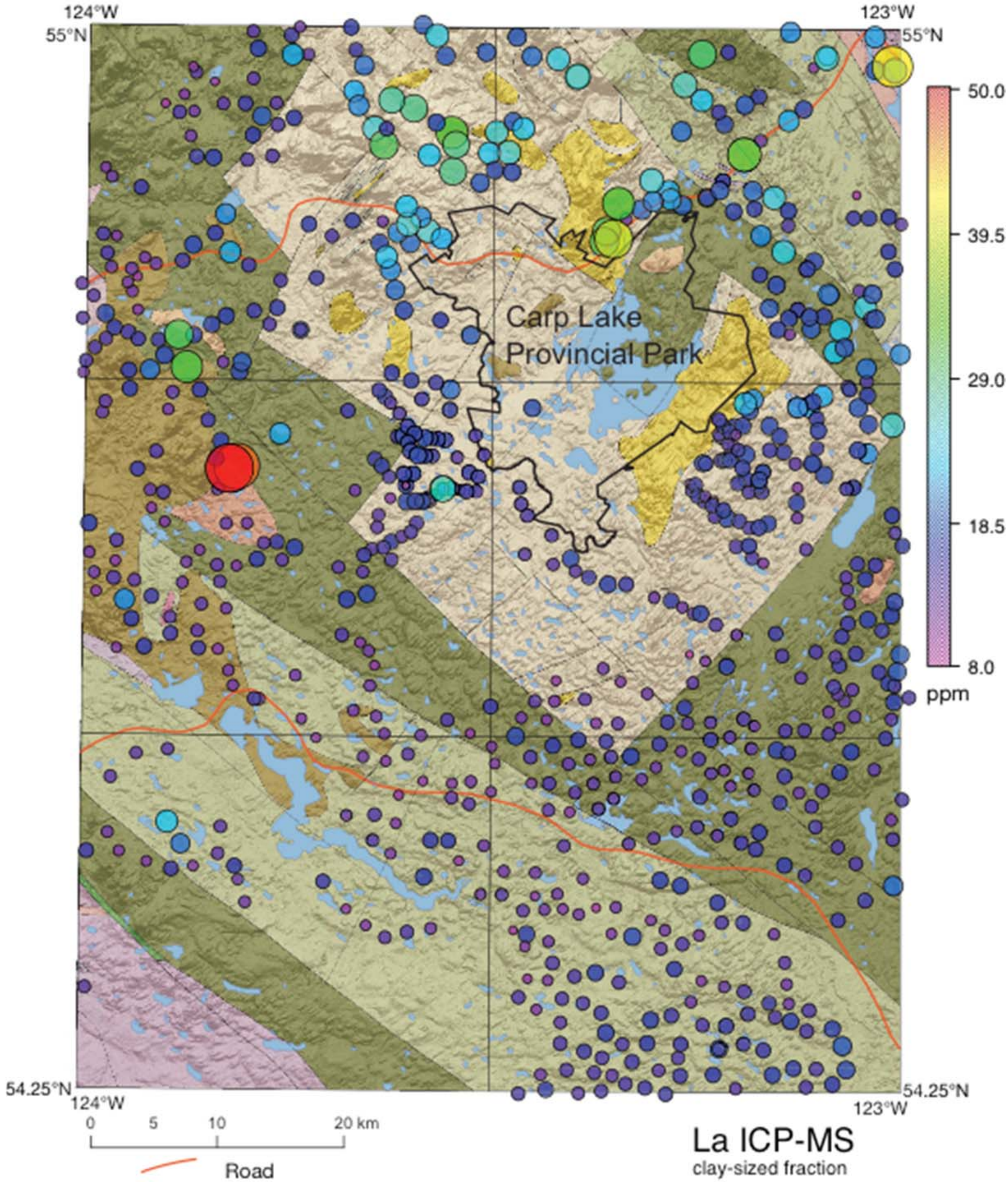

124°W
55°N
123°W
55°N
Carp Lake
Provincial Park
50.0
39.5
29.0
18.5
8.0
ppm
54.25°N
124°W
123°W
54.25°N
0
5
10
20 km
Road
La ICP-MS
clay-sized fraction

Figure 7p

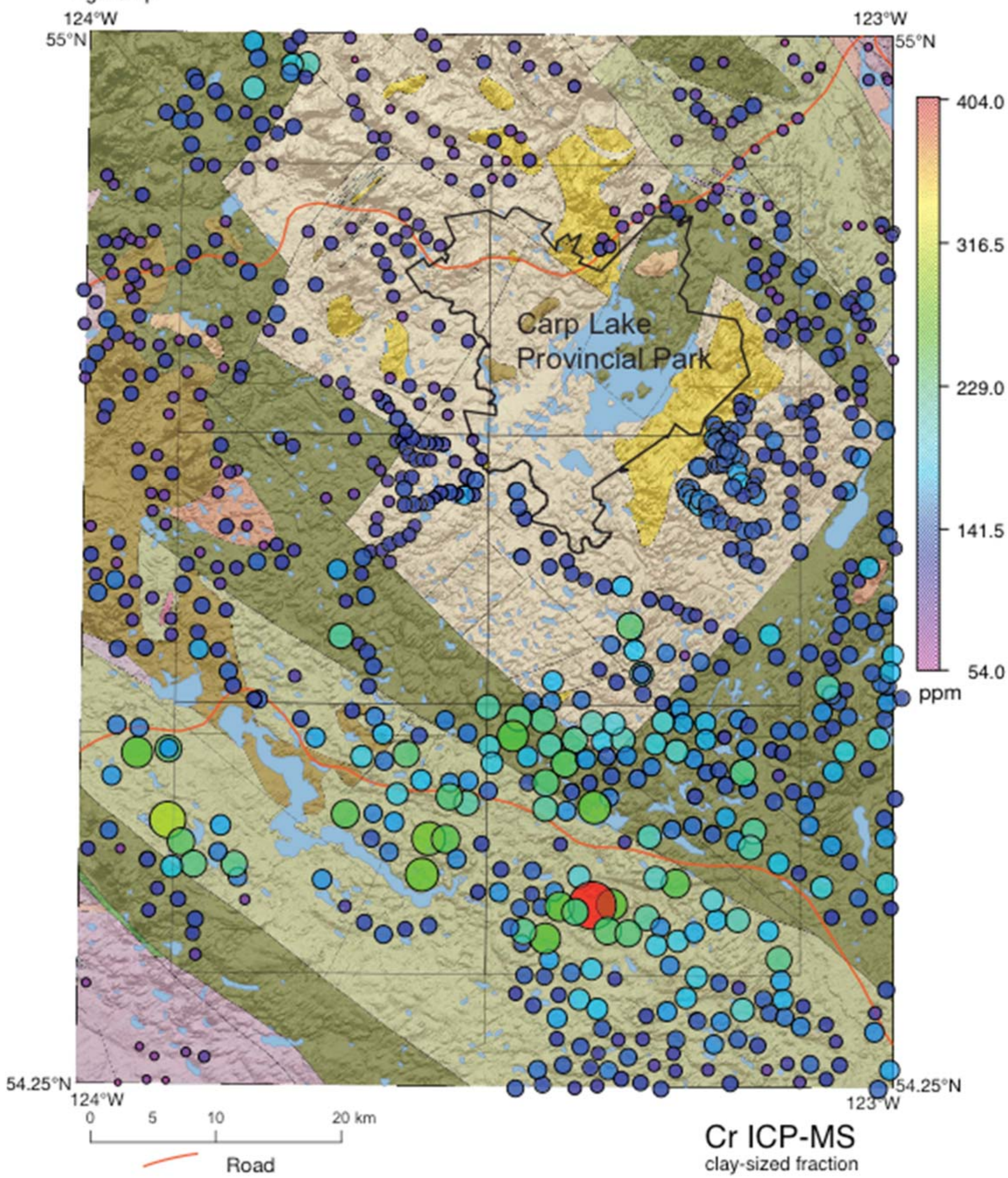

124°W
123°W
55°N
55°N
Carp Lake
Provincial Park
404.0
316.5
229.0
141.5
54.0
ppm
54.25°N
124°W
54.25°N
123°W
0
5
10
20 km
Road
Cr ICP-MS
clay-sized fraction

Figure 7q

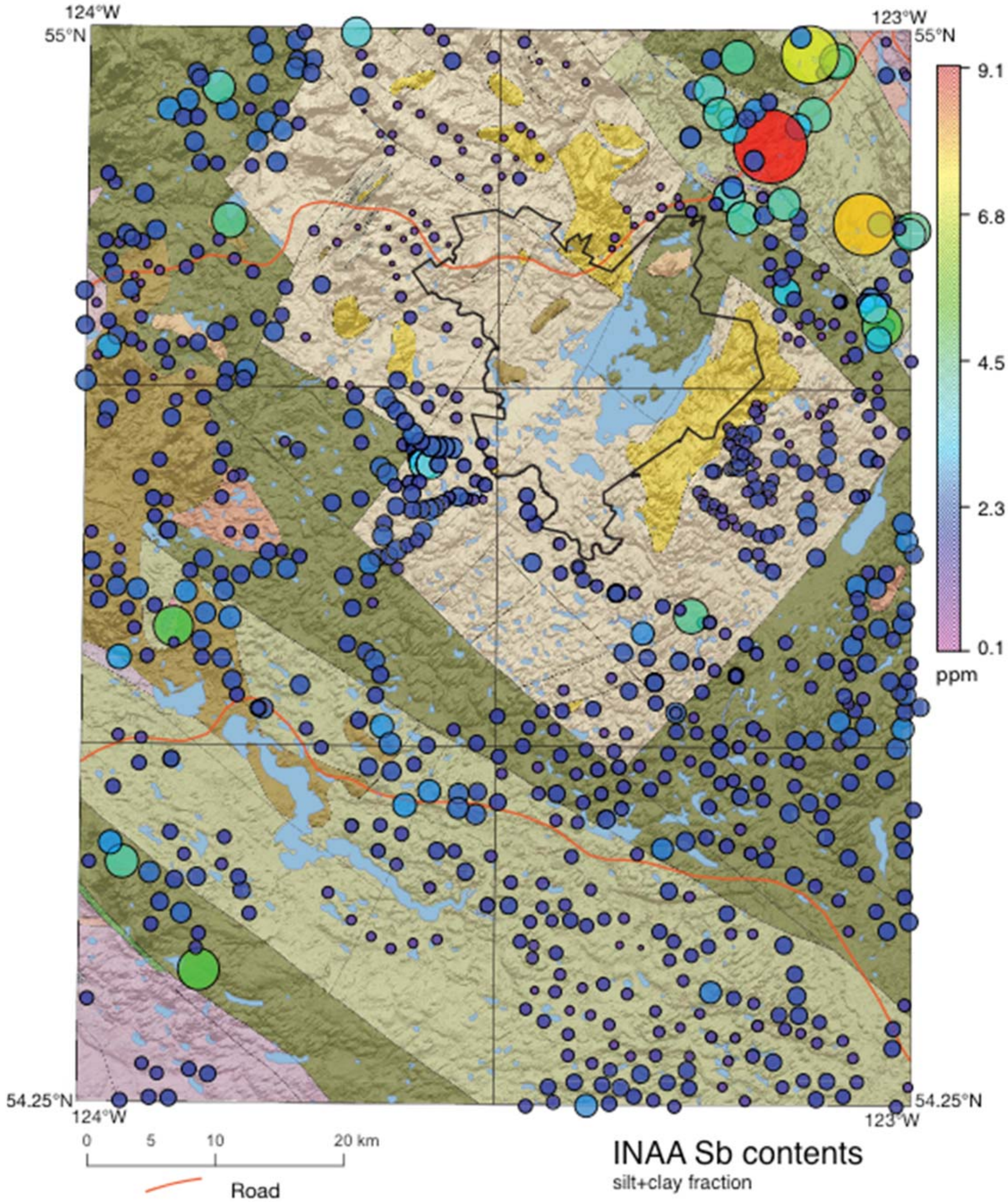

124°W
55°N
123°W
55°N
9.1
6.8
4.5
2.3
0.1
ppm
54.25°N
124°W
54.25°N
123°W
0
5
10
20 km
Road
INAA Sb contents
silt+clay fraction

Figure 7r

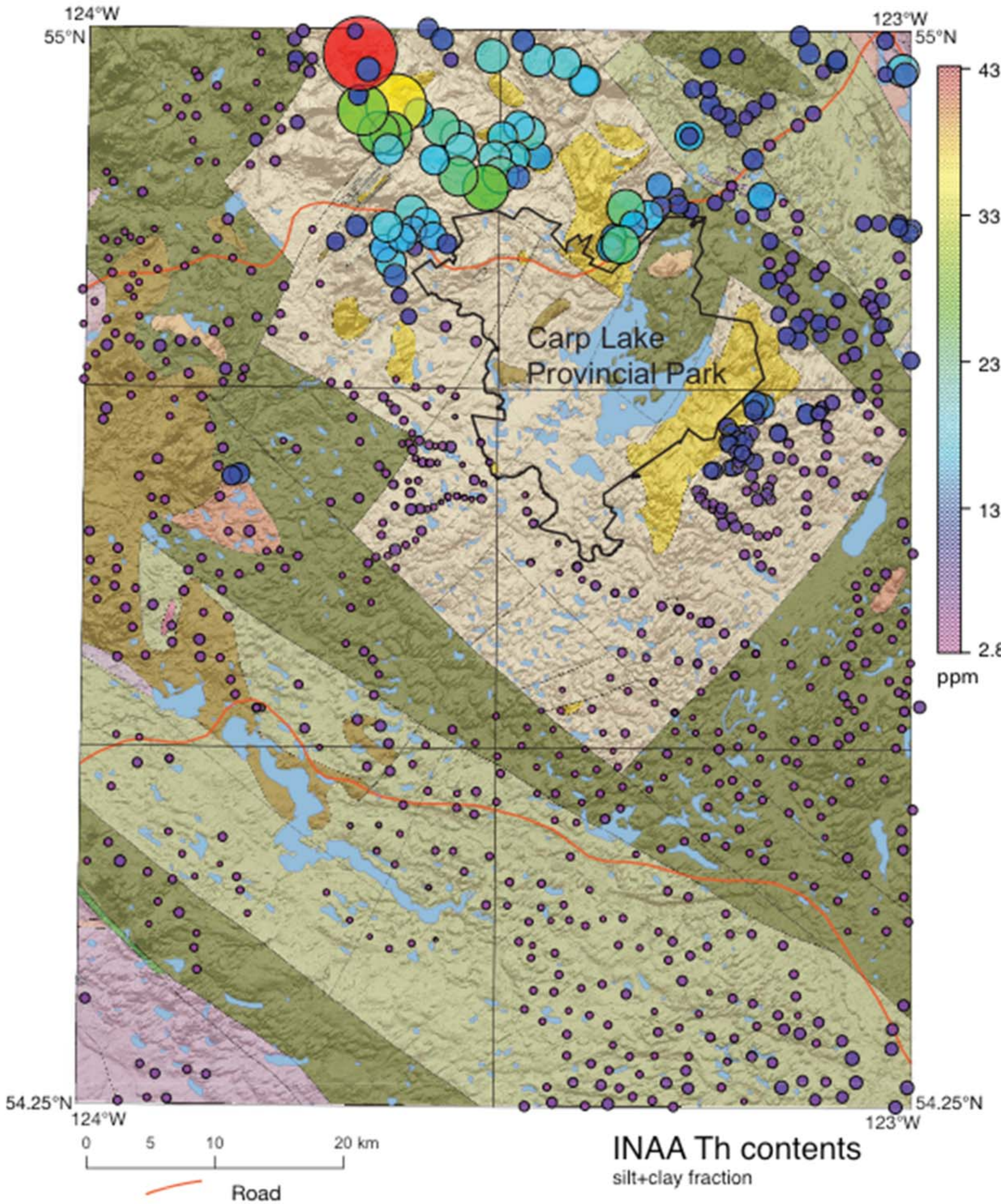
124°W
55°N
123°W
55°N
Carp Lake
Provincial Park
43.0
33.0
23.0
13.0
2.8
ppm
54.25°N
124°W
123°W
54.25°N
0
5
10
20 km
Road
INAA Th contents
silt+clay fraction

Arsenic contents in the heavy mineral fraction range from 9 to 414 ppm and show clearly anomalous values around the 95th percentile (60 ppb) (Figure 6a). The spatial distribution of As contents mimic those of gold and most anomalous values are in the northeast part of the study area with slightly lower values in the northwest (Figure 8c).

Silver contents for the clay fraction range from less than detection (0.1 ppm) to 1.1 ppm (average = 0.21 ±0.14 ppm, n=520), with anomalous values >0.5 ppm (~95th percentile; Figure 6a). Silver shows a moderately positive, statistically significant correlation (r=0.313) with Au, with anomalous values in the northeastern and northwestern parts of the study area (Figure 7e), being coincident with the Au anomalies. Silver for the silt plus clay-size fraction and the heavy mineral fraction was below detection limit for all samples.

Mercury was only detected in the clay fraction, although heavy mineral concentrate data (see below) indicates many samples have significant quantities of cinnabar grains. In the clay fraction, Hg ranges from 0.02 to 1.0 ppm (average = 0.29 ±0.13 ppm). In the cumulative frequency plot there are no major breaks in slope, consistent with a close to normal distribution (Figure 6a). Setting the threshold at the 95th percentile (0.51 ppm), anomalous Hg contents occur in the west-central portion of the study area (Figure 7f), north of the two known Hg showings. Several anomalous Hg contents occur in the northeastern and northwestern parts of the study area, coincident with Au, As and Ag anomalies. Mercury values do not, however, statistically correlate well with Au values (r=0.083), but do statistically correlate moderately with As values (r=0.360).

Cinnabar counts range from 0 to 400 grains. Anomalous cinnabar grain counts (>60 grains) occur in the western part of the study area, and mark the start of a trend of decreasing values to the southeast (Fig. 8e). Because of the large number of cinnabar grains identified, the 2009 and 2010 samples were also analyzed for Hg by INAA; unfortunately, because of detection limit issues due to interference with other elements, only 14 samples have values above detection. These samples are on the west and east side of the study area and do mimic highs in the cinnabar grain counts (Fig. 8f).

Cu, Mo and Sb in Till

Copper was analyzed only for the clay fraction samples and ranges from 33 to 408 ppm (average = 125 ±38 ppm). Based on the cumulative frequency plot, Cu contents in the clay fraction are anomalous at the 90th percentile (165 ppm; Figure 6a). Anomalous Cu contents occur in the northwestern corner of the study area, with smaller anomalies in the northeastern

Figure 8 (next 10 pages): Proportional dot maps of selected elements and minerals for <0.25 mm fraction of till heavy mineral separates for INAA geochemical analyses along with selected grain counts. ***a)*** *Gold grain counts,* ***b)*** *Au,* ***c)*** *As,* ***d)*** *Sb,* ***e)*** *cinnabar,* ***f)*** *Hg,* ***g)*** *Ce,* ***h)*** *Th,* ***i)*** *Cr, and* ***j)*** *pyrite. Size of dots are proportional to the content with Au, Cinnabar, and pyrite grains, and Au, As, and Th being represented by log plots. Data are overlaid on the bedrock geology map presented in Figure 2.*

Figure 8a

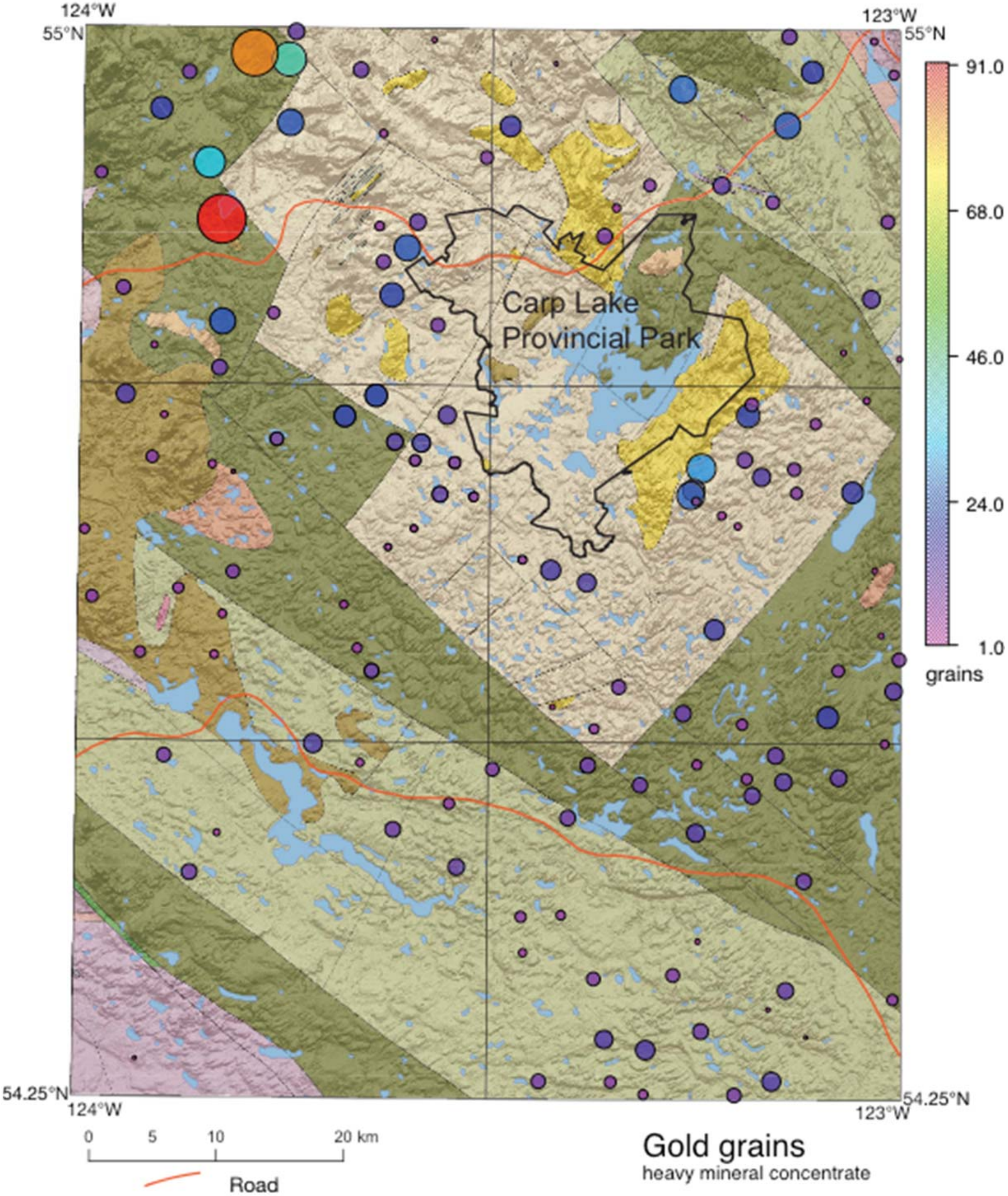

124°W
55°N
123°W
55°N
Carp Lake
Provincial Park
91.0
68.0
46.0
24.0
1.0
grains
54.25°N
124°W
123°W
54.25°N
0
5
10
20 km
Road
Gold grains
heavy mineral concentrate

Figure 8b

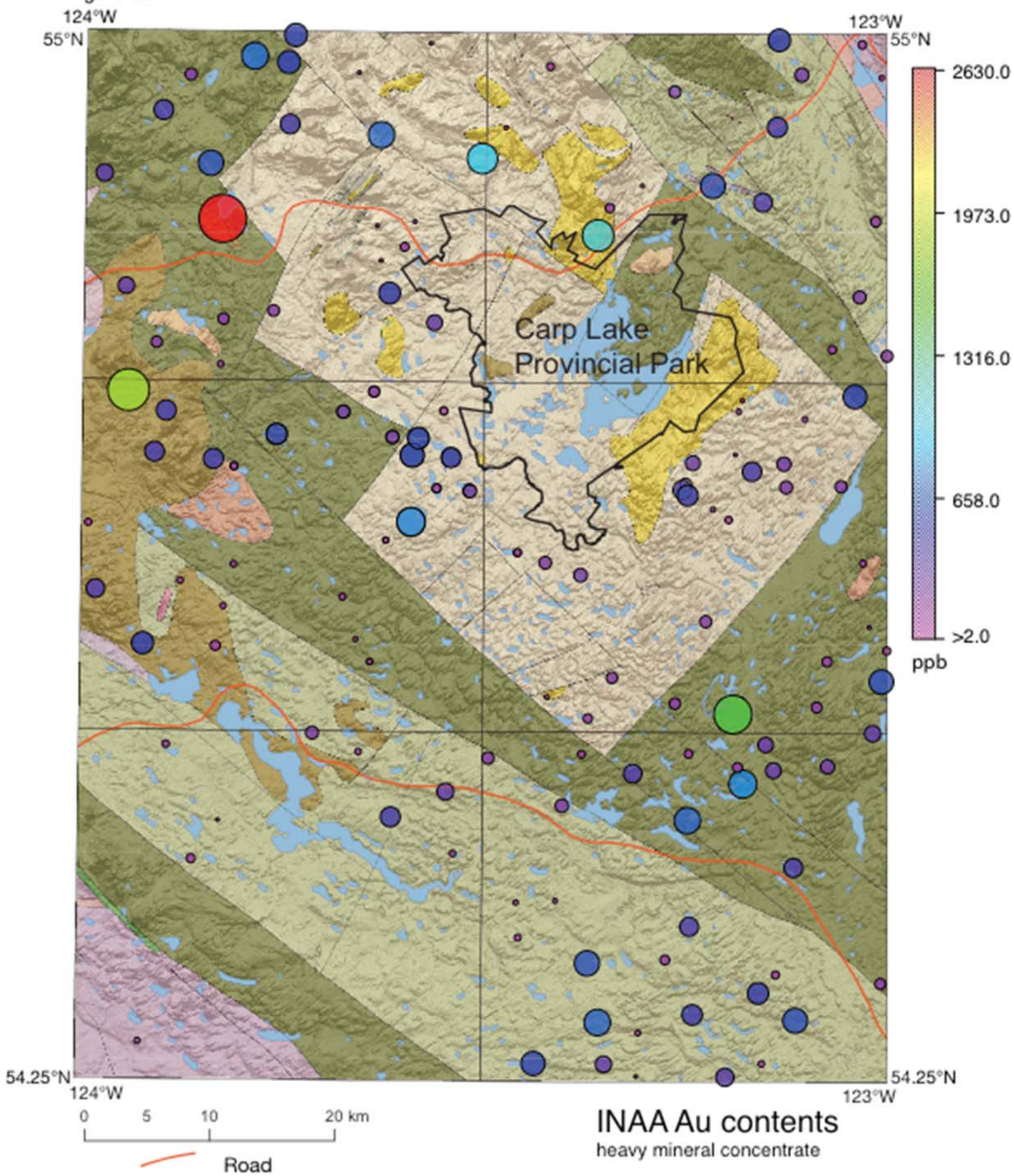

124°W
55°N
123°W
55°N
2630.0
1973.0
1316.0
658.0
>2.0
ppb
Carp Lake
Provincial Park
54.25°N
124°W
54.25°N
123°W
0
5
10
20 km
Road
INAA Au contents
heavy mineral concentrate

Figure 8c

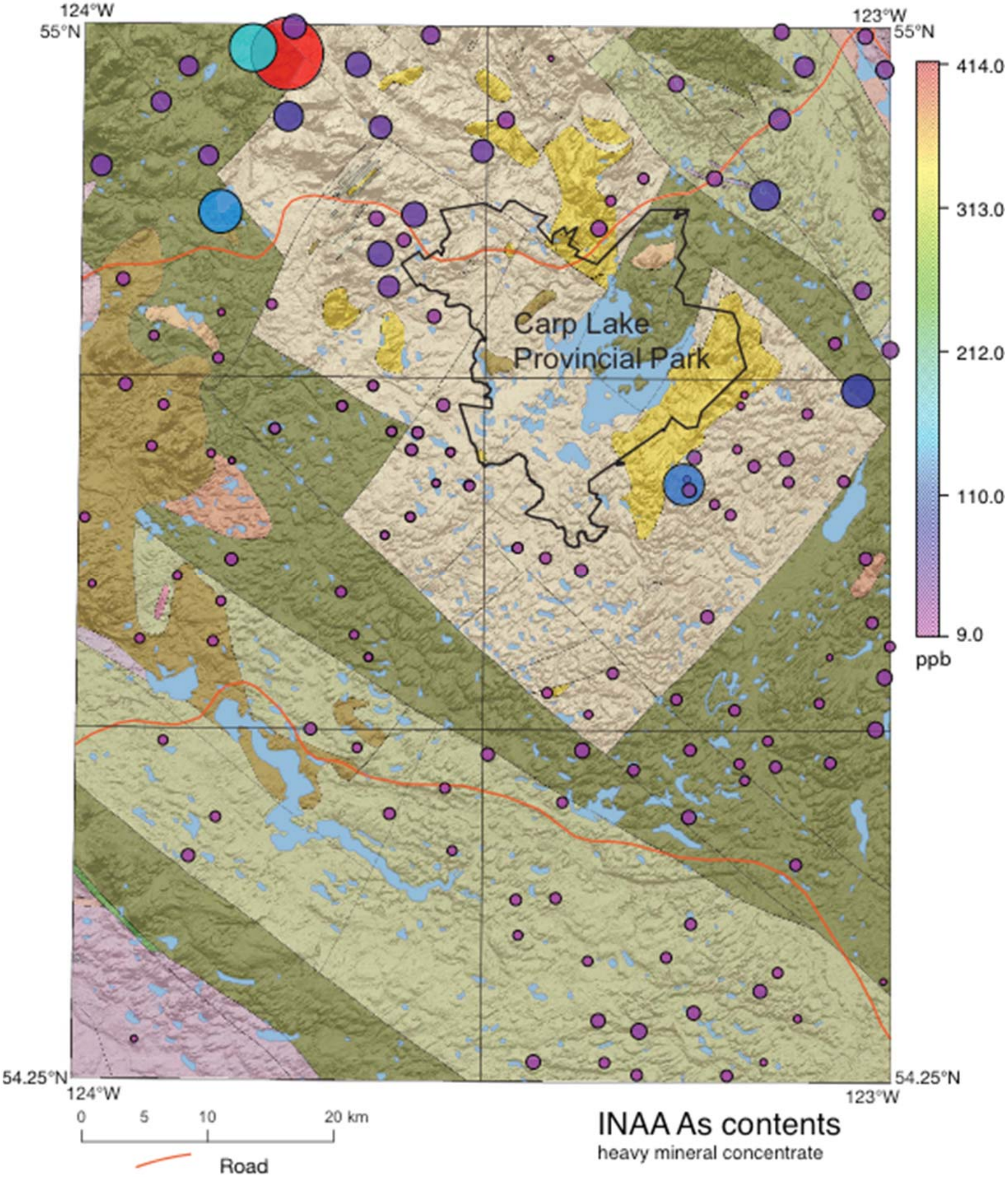

124°W
55°N
123°W
55°N
Carp Lake
Provincial Park
414.0
313.0
212.0
110.0
9.0
ppb
54.25°N
124°W
54.25°N
123°W
0
5
10
20 km
Road
INAA As contents
heavy mineral concentrate

Figure 8d

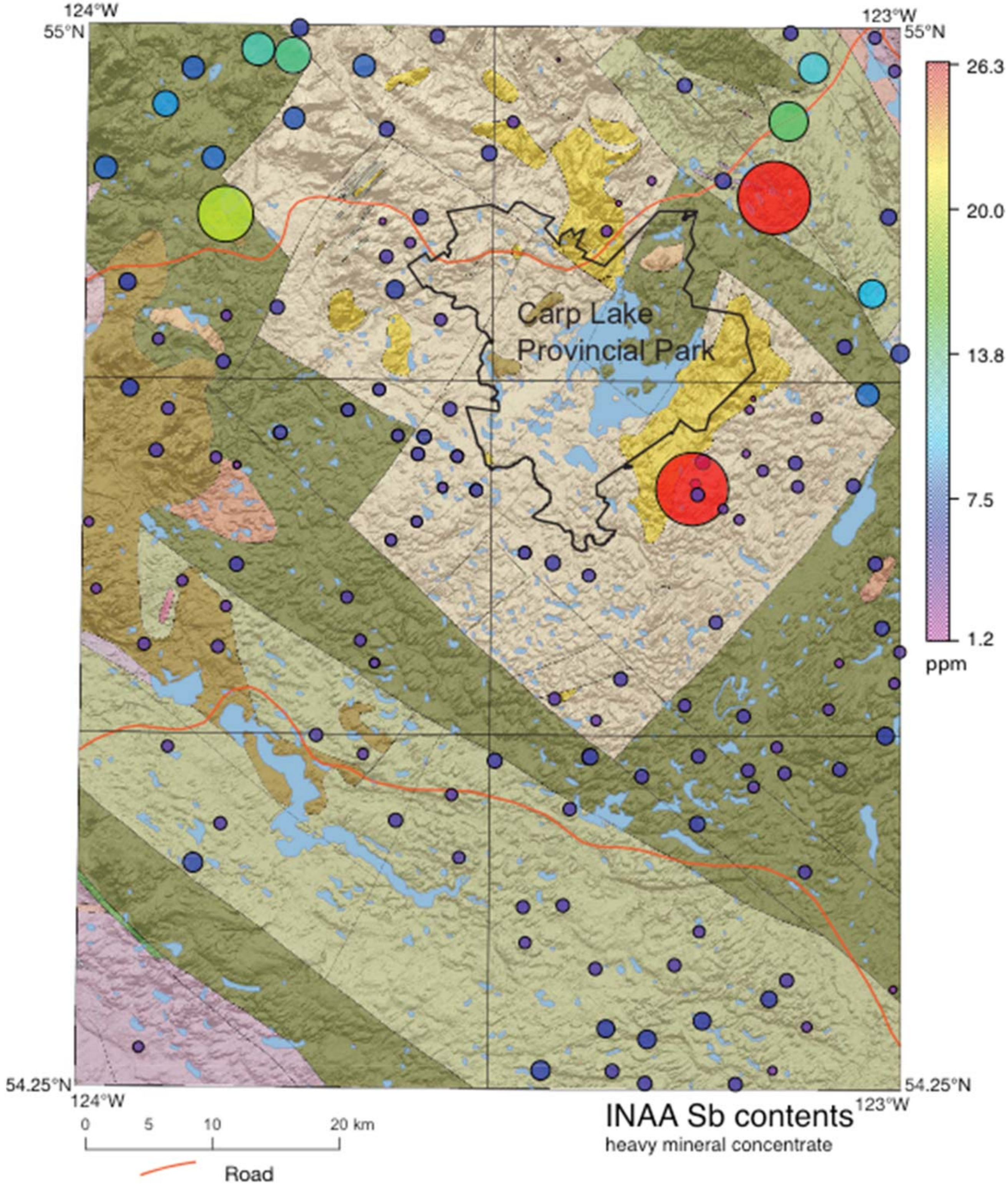

124°W
55°N
123°W
55°N
Carp Lake
Provincial Park
26.3
20.0
13.8
7.5
1.2
ppm
54.25°N
124°W
54.25°N
123°W
0
5
10
20 km
Road
INAA Sb contents
heavy mineral concentrate

Figure 8e

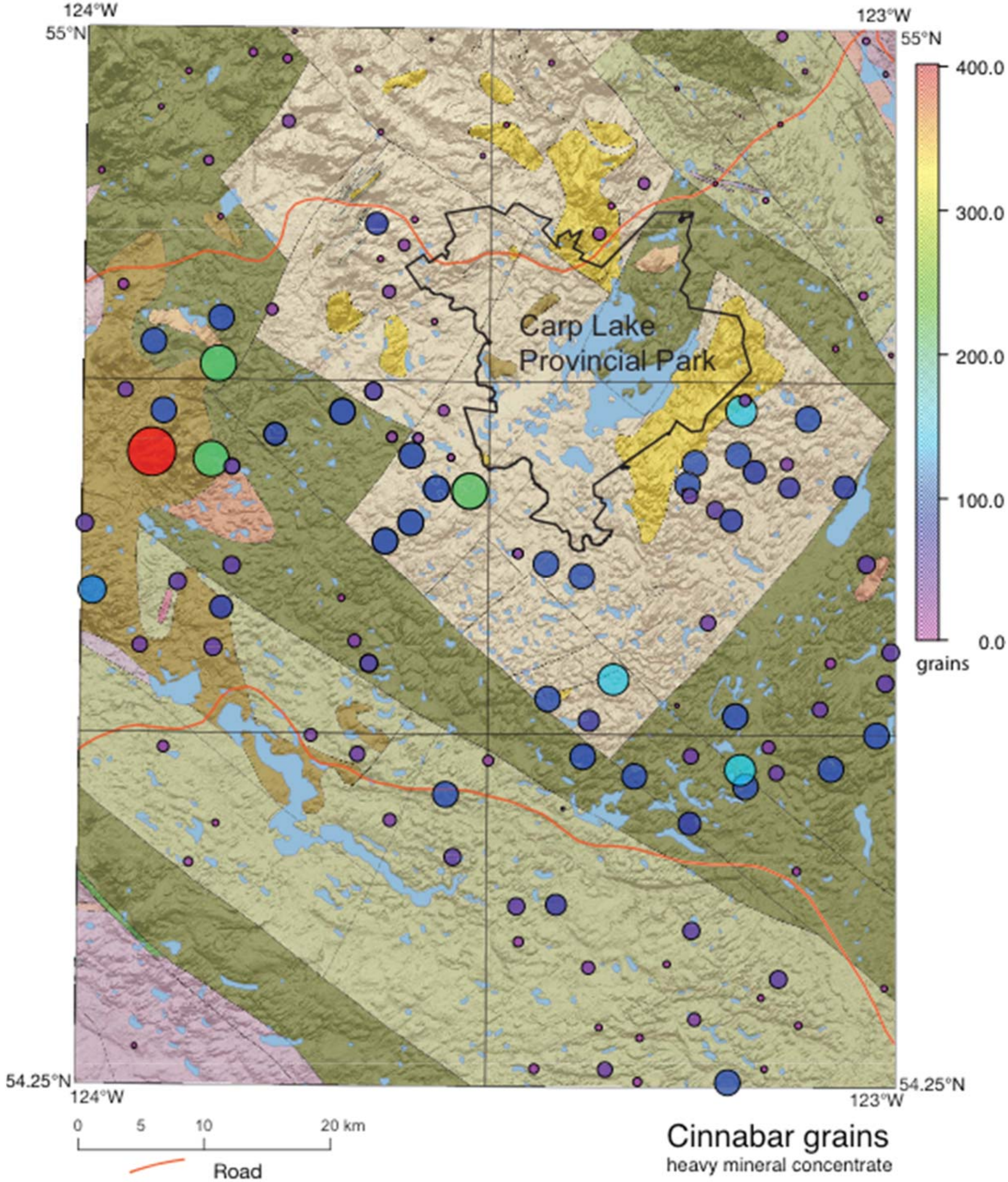
124°W
123°W
55°N
55°N
54.25°N
54.25°N
124°W
123°W
Carp Lake
Provincial Park
400.0
300.0
200.0
100.0
0.0
grains
0
5
10
20 km
Road
Cinnabar grains
heavy mineral concentrate

Figure 8f

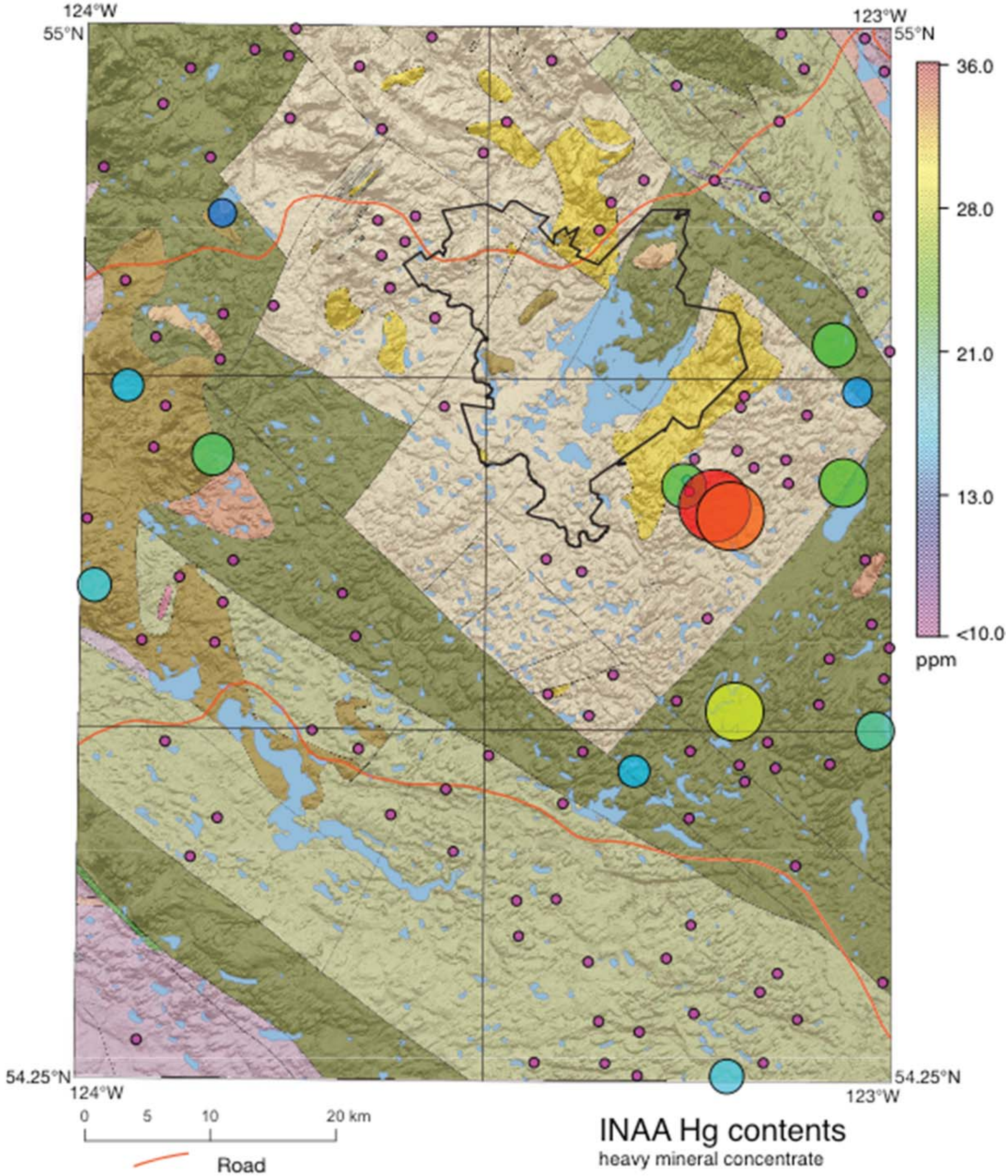

124°W
55°N
123°W
55°N
36.0
28.0
21.0
13.0
<10.0
ppm
54.25°N
124°W
54.25°N
123°W
0
5
10
20 km
Road
INAA Hg contents
heavy mineral concentrate

Figure 8g

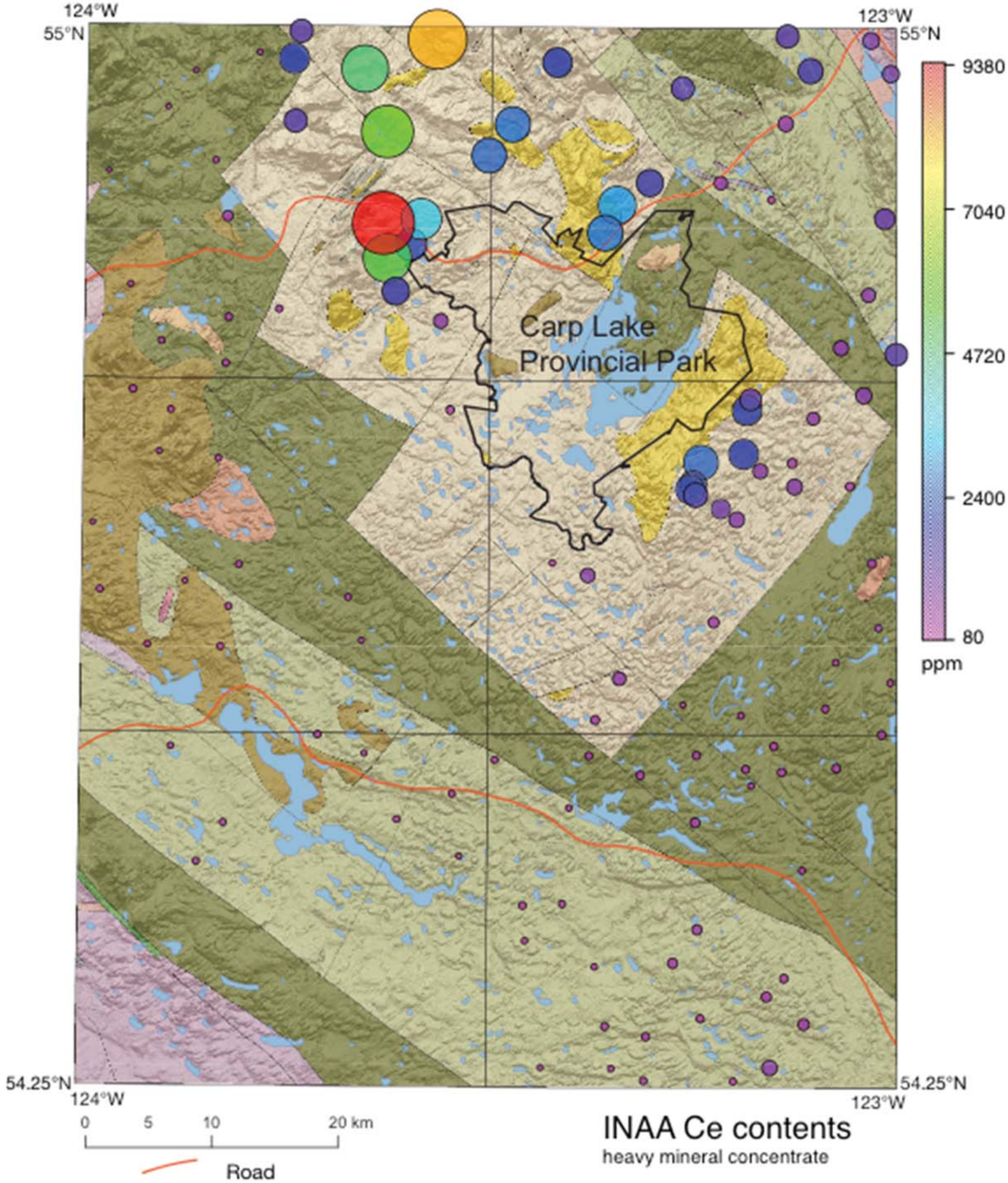

124°W
55°N
123°W
55°N
Carp Lake
Provincial Park
9380
7040
4720
2400
80
ppm
54.25°N
124°W
123°W
54.25°N
0
5
10
20 km
Road
INAA Ce contents
heavy mineral concentrate

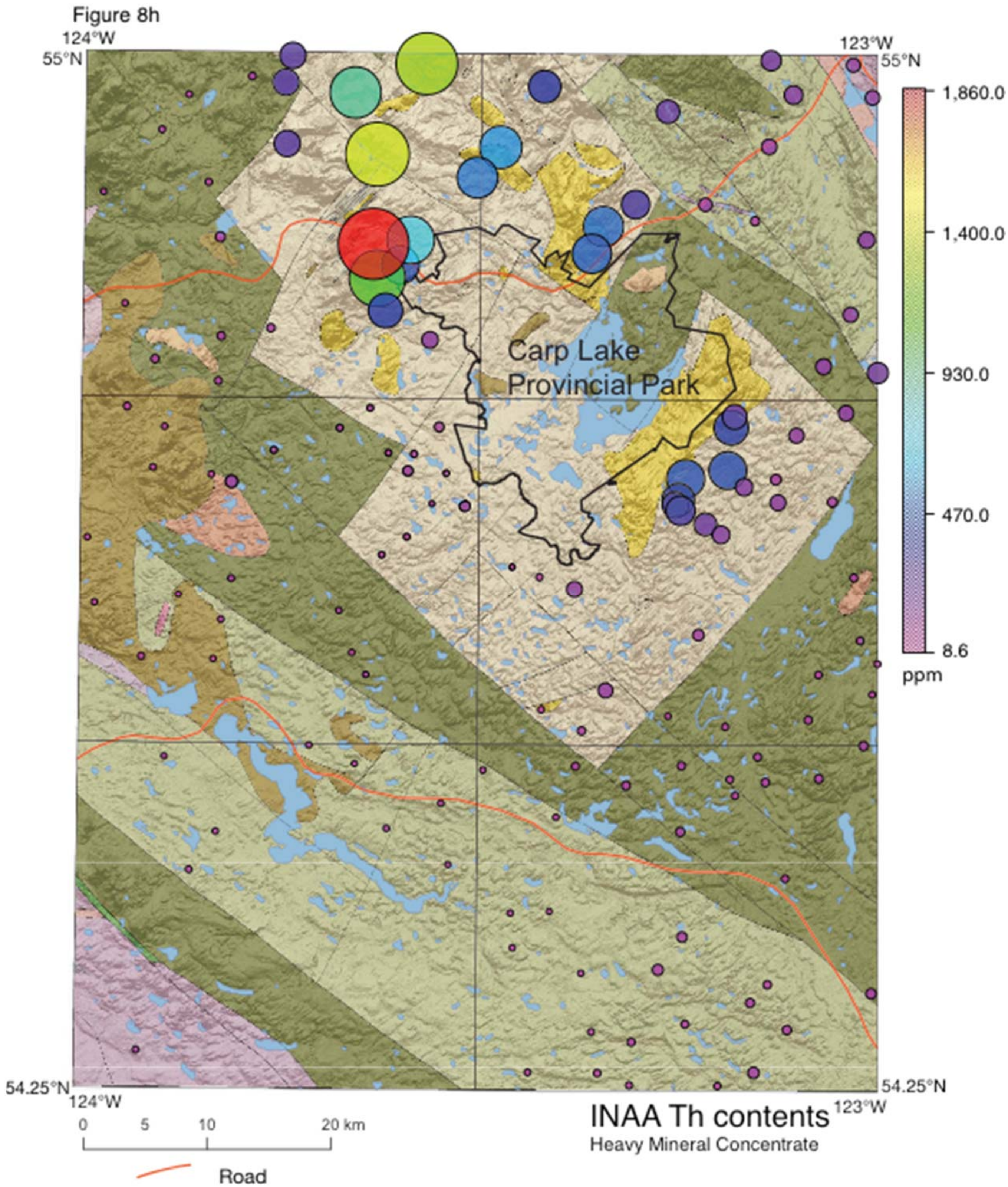

Figure 8h
124°W
55°N
123°W
55°N
1,860.0
1,400.0
930.0
470.0
8.6
ppm
Carp Lake
Provincial Park
54.25°N
124°W
54.25°N
123°W
0
5
10
20 km
Road
INAA Th contents
Heavy Mineral Concentrate

Figure 8i

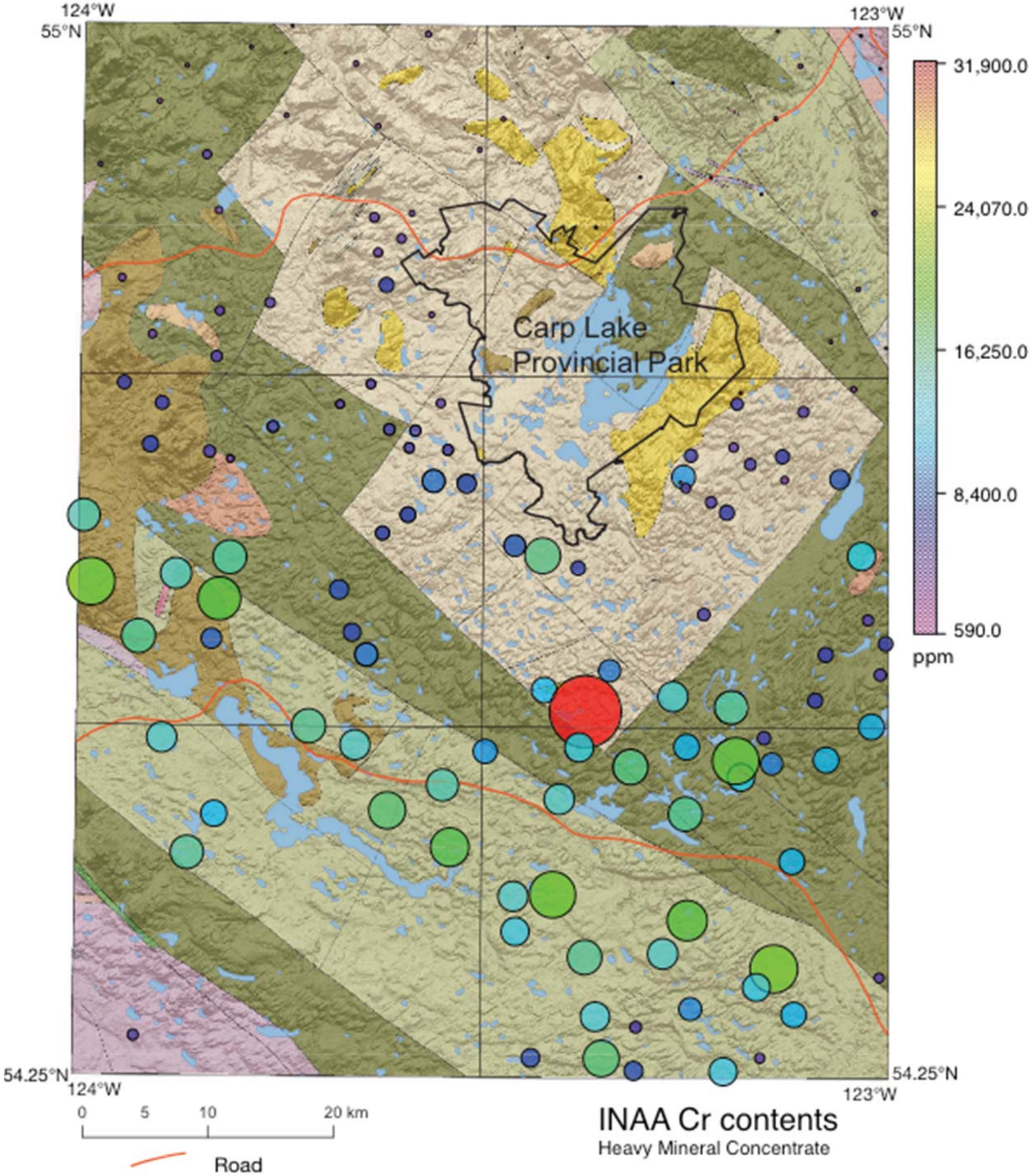
124°W
55°N
123°W
55°N
Carp Lake
Provincial Park
31,900.0
24,070.0
16,250.0
8,400.0
590.0
ppm
54.25°N
124°W
54.25°N
123°W
0
5
10
20 km
Road
INAA Cr contents
Heavy Mineral Concentrate

Figure 8j

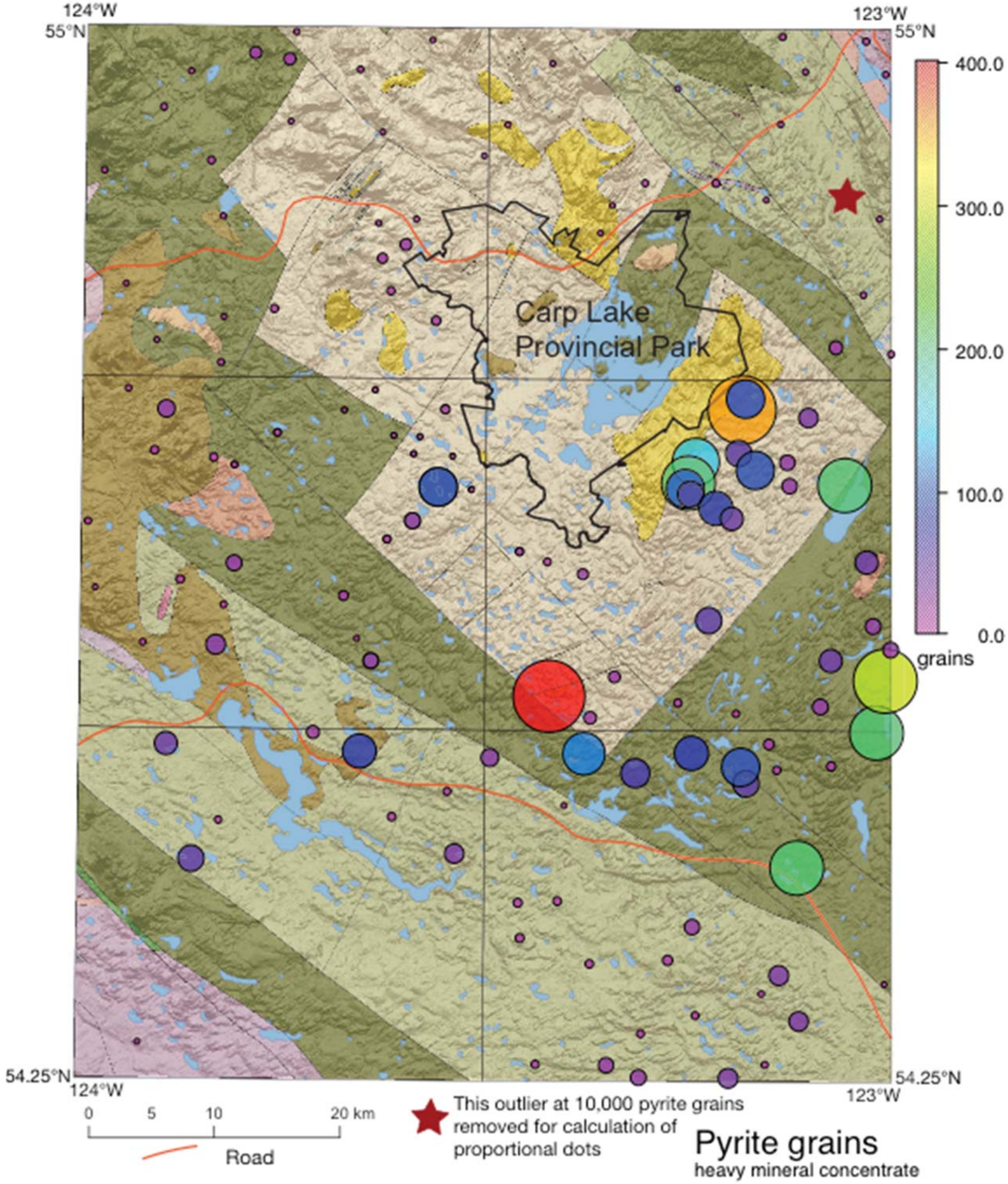

124°W
55°N
123°W
55°N
400.0
300.0
200.0
100.0
0.0
grains
Carp Lake
Provincial Park
54.25°N
124°W
54.25°N
123°W
0
5
10
20 km
Road
This outlier at 10,000 pyrite grains removed for calculation of proportional dots
Pyrite grains
heavy mineral concentrate

corner (Figure 7g). There is a positive concentration correlation between Cu and a number of other analytes such as Fe (r=0.712), Sc (r=0.654), V (r=0.656), As (r=0.538), Au (r=0.410), Co (r=0.341) and Mo (r=0.313). These element associations indicate that Cu in the clay fraction of the till in the northwestern and northeastern parts of the study area is associated with Cu-Au mineralization.

Molybdenum was analyzed for both size fractions. All clay samples returned Mo contents above the detection limit, ranging from 0.3 to 12 ppm (average = 1.74 ±1.12 ppm). By contrast, the silt plus clay-size fraction had only 137 samples above detection limit (1 ppm), ranging from 3 to 28 ppm. For the clay fraction, the anomalous threshold is around the 97th percentile (3.5 ppm; Figure 6a), whereas for the silt plus clay-size fraction, all samples with detectable Mo can be considered anomalous at the 85th percentile (≥3 ppm; Figure 6a). The two size fractions show different spatial relationships. For the clay fraction, anomalous Mo contents occur mainly in the northeastern section of the study area; Mo contents are not anomalous in the northwestern section (Figure 7h). The highest Mo content is for a sample in the west-central part of the study area. By contrast, the silt plus clay-size fraction has anomalous Mo contents scattered over much of the study area, with the most consistently elevated contents in the east-central and southern areas. Notably, Mo contents in the silt plus clay-size fraction are below detection for the northwestern area where high Cu, Au and As values occur.

Antimony was measured for both size fractions, with clay contents ranging from 0.1 to 5.6 ppm (average = 0.80 ±0.48 ppm), and clay+silt contents ranging from 0.5 to 13.1 ppm (average = 1.84 ±0.87 ppm). Threshold values are around the 95th percentile for both fractions, at 1.5 and 2.7 ppm for the clay and silt plus clay-size fractions, respectively (Figure 6a). Spatially, the two size fractions show similar distributions, with the most anomalous contents occurring in the northeastern section of the study area (Figure 7i). Antimony is also a common pathfinder element of porphyry Cu-Au and VMS mineralization. Antimony in the heavy mineral fraction ranges from 1.2 to 26.3 ppm, and is anomalous at the 90th percentile (~7 ppm) (Figure 6a). The two highest values in the heavy mineral fraction are to the southeast and northeast of Carp Lake, with intermediate values in the northwest, the zone of potential porphyry Cu-Au style mineralization.

Pb, Bi, Zn and Cd in Till

Lead was only analyzed in the clay fraction, and ranges from 6.6 to 64 ppm (average = 15.0±5.21 ppm). Lead shows a near normal distribution, although there is a subtle inflection in the cumulative frequency plot near the 85th percentile (Figure 6a); setting the threshold value at the 95th percentile gives anomalous Pb at >24 ppm. The strongest correlations with Pb are shown by K (r=0.591), La (r=0.501), Bi (r=0.668), Th (r=0.720) and U (r=0.621). The spatial distribution of anomalous Pb concentrations is distinct from the other commodity-related elements, with the highest Pb contents in the north-central part of the map area, between the northeastern and northwestern areas that are anomalous in Au, Cu and As (Figure 7j). Bismuth (Figure 7k) shows a similar spatial distribution to Pb, along with U, Th and the rare earth elements (REE). Bismuth ranges from less than detection (0.1 ppm) to 2.7 ppm (average = 0.33 ±0.26 ppm), with a threshold around the 95th percentile (0.8 ppm; Figure 6b).

Zn contents were analyzed in both size fractions and Cd was only analyzed in the clay fraction. Zinc contents in clay range from 83 to 531 ppm (average = 187 ±41 ppm) compared to 60 to 400 ppm in the clay+silt (average = 167 ±49 ppm, with around 280 samples below detection). Cadmium shows similar spatial distribution to Zn, and ranges from 0.1 to 4.0 ppm (average = 0.75 ± 0.48 ppm). Both metals show the largest anomalies (threshold at the 95th percentile = 245 ppm Zn for clay, 250 ppm Zn for clay+silt and 1.6 ppm Cd for clay; Figure 6b) along the eastern side of the map area (Figure 7l, m), although Cd also shows several anomalous values in the west-central portion of the study area. Both Zn and Cd have strong positive correlations with Mo (r=0.743 and 0.586, respectively), As (r=0.421 and 0.364, respectively) and Sb (r=0.464 and 0.334, respectively), as well as with each other (r=0.719). Although Zn correlates poorly with major elements, Cd is strongly correlated with Ca (r=0.595).

Rare Earth Elements, U, Th, K, Ca, Mg, Na, Cr, Hf, Co, Mn and Ni in Till

Both the basal till geochemical results and the INAA determinations on the heavy mineral fraction show that values for rare earth elements (REE), U, Th, K, Ca, Mg, Na, Ni, and Cr (only La, Th and Cr shown in Figure 7 as examples) have spatial relationships that are consistent with changes in the dominant underlying bedrock lithology (e.g., Figures 7n, o, p). Thus, incompatible elements that are enriched in felsic rocks (i.e., the REE, U, Th, K and Hf) are elevated in the northern part of the study area coincident with the Wolverine metamorphic complex, which contains felsic rocks such as granitic pegmatite, granite, granodiorite and rhyolite (Struik, 1994). In the large HMC samples from this area of the map, >33% of the clasts that are >2 mm are granitoid, indicating a greater prevalence of alkalic volcanic rocks and associated late stage intrusive rocks. Nickel and Cr contents are highest in the south-southwest portion of the study area where mafic and volcaniclastic rocks of the Quesnel Terrane occur (Struik, 1994). Conversely, whereas Co shows a strong correlation with Mn in the clay fraction, Cr and Ni, which are strongly adsorbed by Mn oxides and oxyhydroxides (Nicholson and Eley, 1997; Leybourne et al., 2003), show distribution patterns that follow the major mafic volcanic bedrock units in the southern part of the study area (Figure 7p). High Ta, Ce and Th contents in the north to northeast suggest more felsic rocks, likely the granitic pegmatite, granite, granodiorite and rhyolite and/or more enriched mafic rocks; whereas high Cr contents in the south indicates more primitive mafic rocks (Figures 7g, h, i, j).

Heavy Mineral Concentrates: visible gold, pyrite and cinnabar

All till samples processed for heavy minerals (n=152) contain visible gold grains. The number of gold grains per ~10 kg of sample ranges from 1 to 91 (Figure 8a) and the calculated Au contents range from 1 to 23,491 ppb. In total, 1584 gold grains were classified on the basis of size and morphology. Gold grain morphologies are subdivided into three groups: pristine, modified and reshaped, based on the classification scheme of Dilabio (1990). The majority of gold grains in this study are classified as reshaped (82.5%), with less common modified grains (14%) and rare pristine grains (3.5%). The threshold value for the total number of gold grains is around 12–15 (80–85th percentile), based on changes in slope of a probability distribution.

Although they are only estimates, grain counts of pyrite and cinnabar are useful. Pyrite counts range from zero to a high of ~10 000 grains. Most of the till samples with elevated pyrite grain counts (where anomalous values are approximately >50 grains) occur in the eastern and southern parts of the study area (Figure 8b), distinctly south of the area with anomalous metal values (northeastern corner of the study area; Figures 7a–i, k–m). By contrast, cinnabar counts range from 0 to 400, with anomalous cinnabar grain counts (approximately >60 grains) in the western part of the study area, with a trend of decreasing values to the southeast (Figure 8c).

TILL GEOCHEMICAL EXPLORATION

Precious and base metal veins

In the northeastern part of the study area, there are a number of Au and Cu-Au showings, as well as two small past-producing placer deposits (discussed previously). Historic gold recovered from the placer deposits was described as wiry to angular (MINFILE 093J 007), suggesting that the placer gold had not been transported far from source. Samples of the clay fraction were analyzed by aqua-regia digestion followed by ICP-MS, whereas the silt plus clay-size fraction was analyzed by INAA, thus the ICP-MS results will be less biased by the nugget effect. Gold in the clay fraction occurs either as clay-sized gold grains, most likely a result of glacial comminution and/or small-scale hydromorphic gold dispersion and adsorption to clay and oxyhydroxide mineral surfaces in the clay fraction. Other than a small number (~3) of highly anomalous Au values in the ICP-MS results, there is a relatively strong correlation (r=0.410) between Cu and Au; this suggests that much of the Au is associated with Cu-sulphide minerals. The pathfinder elemental associations presented here (i.e., Sb, As, Se, Tl, Cd, Zn) are consistent with this style of mineralization (Taylor, 2007). This association is coherent with descriptions of many of the showings in the northeastern section of the study area; showings of quartz veins with Au, Cu±Ag and/or PGE (MINFILE 093J 007, 093J 012, 093J 027, 093J 037), likely of epigenetic origin. The main cluster of till samples with anomalous values is essentially spatially coincident with many of the showings. The dominant ice flow towards the northeast can be used as a vector to guide further prospecting.

Porphyry Cu-Au

There is potential for porphyry Cu-Au–style mineralization in the study area based on the presence of the Mount Milligan porphyry Cu-Au developed prospect in correlative rocks to the northwest of the study area. The till geochemical data shows elevated values of Cu and Au and a number of pathfinder elements (e.g., As, Hg, Sb) in the northwestern part of the study area (Figures 7a, b, c, d, f, g, i). These anomalous till samples strongly indicate sources of mineralization up-ice, towards the southwest. There are a number of Cu and Cu-Au showings coincident and up-ice of this area of elevated geochemical values (Figure 2). For example, at the Tsil showing (MINFILE 094C 180), in the northwestern corner of the study area, there are reports of outcrops of intermediate hornblende and feldspar porphyritic rocks exhibiting quartz-carbonate alteration with pyrite, pyrrhotite and rare chalcopyrite veins. The main cluster of Cu and Au anomalies in the northwestern part of the study area directly overlie the main cluster of Cu and Au showings in this area (Figure 2).

The highest heavy mineral contents correspond to the area identified as having potential porphyry Cu-Au style mineralization (cf. Ward et al., 2011).

Volcanogenic Massive Sulphide Deposits

Volcanogenic massive sulfide showings occur to the southeast and to the northwest of the study area along the trend of the major bedrock units. Given the presence extensive volcanic rocks, there should be significant potential for VMS mineralization in the study area, even though there are no VMS showings or deposits listed in MINFILE. However, this study indicates there is relatively little spatial correlation between the commodity elements associated with VMS mineralization. Lead anomalies are clearly distinct from both Cu and Zn. The relatively low Pb contents in the till in the study area, compared to other areas of VMS deposits (cf., Hall et al., 2003; Parkhill and Doiron, 2003), could be related to three factors:

- Given the preponderance of mafic volcanic rocks in this part of BC, VMS mineralization, if present, would likely be lead-poor given the generally juvenile nature of the source of the volcanic rocks (Smith et al., 1995; Patchett and Gehrels, 1998; Dostal et al., 1999; Erdmer et al., 2002; Ross et al., 2005). Furthermore, VMS deposits associated with ocean floor and oceanic arc settings are lead-poor compared to those associated with continental margins (Franklin et al., 1981; Galley et al., 2007).
- Only the clay fraction was analyzed for Pb, by aqua-regia digestion followed by ICP-MS, and it is possible that Pb is present in a less labile form or in a coarser size fraction.
- It is possible that the thick till units of the study area have diluted the geochemical signature of underlying bedrock lithologies resulting in subdued anomalies for Pb.

Despite an apparent lack of geochemical response for Pb in till samples there is still potential for VMS-style mineralization in the study area. The general lack of spatial correlation between anomalous Cu and Zn may simply be a function of VMS-related Cu anomalies being masked by anomalies associated with porphyry Cu-Au and precious and base metal vein mineralization or by dilution due to thick till. Zinc shows poor correlations with Ni, Cr and Mg indicating that anomalous Zn contents in the till are not simply a function of weathering of mafic volcanic rocks. In addition to anomalous Zn along the eastern portion of the study area (Figure 7l), there are coincident anomalies for Cd, Bi and Tl, suggesting the potential for concealed, presently unrecognized, Zn mineralization. The HMC samples with the highest pyrite grain counts are also from the east-central part of the map area (Figure 8b), further suggesting the presence of VMS-style mineralization in this area. More detailed work following up the source of anomalous pyrite grain counts and Zn, Cd, Bi and Tl contents in the till is warranted.

Mercury

Pinchi Lake mercury mine (MINFILE 093K 049) is located on the Pinchi fault approximately 45 km to the northwest of the two Hg occurrences in the southwestern portion of the study area (Figure 2). The Pinchi Lake mine operated from 1940 to 1944 and 1968 to 1975, and was one of only two mercury-producing mines in Canada (Plouffe, 1998). The two Hg showings within the study area are associated with the extension of the Pinchi fault, but anomalous cinnabar counts and Hg contents in the clay fraction are not spatially associated with these showings (Figures 7f, 5c). Elevated cinnabar grain counts occur to the north of the showings, suggesting additional sources of fault-associated Hg mineralization up ice from the cinnabar grains. Moderately elevated Hg in the clay fraction also occurs in the area of high cinnabar grain counts. Follow-up work that includes an analysis of the silt plus clay-size fraction using an analytical method with lower detection limits for Hg is warranted.

HEAVY MINERAL CONCENTRATE GEOCHEMISTRY

The INAA determinations on heavy mineral concentrates presented here add to the previously published data and begin to build a coherent story on the potential for metallic mineralization in the study area. The spatial distribution of Au, As and Sb contents confirm the potential for precious and base metal vein mineralization and to a lesser extent porphyry Cu-Au in the northeast and northwest areas of the study area, respectively. With greater than 30 samples having Au contents greater than 400 ppb, there is the potential for mineralized bedrock to occur there. Gold anomalies commonly coincide with anomalies in other pathfinder elements such as As and Sb. Although only a limited number of values are above detection limit, the spatial distributions of Hg values in the heavy mineral concentrates do mimic the cinnabar grain counts. Areas with elevated INAA values and grain counts may be associated with faults similar to the Pinchi Lake fault.

Elevated light REEs and Th in the northern part of the study area are coincident with, and located down-ice from, granite pegmatite, granite, and granodiorite suggesting the possibility of REE mineralization being associated with felsic porphyry bodies in the area. Our previous studies on the clay+silt and clay fractions of study area tills and the presence of large numbers of pyrite/marcasite grains in some of the HMC samples suggest possible VMS mineralization (Ward et al., 2011). However, the inherent limitations of the INAA method (e.g., lack of Cu and Pb determinations and high detection limits for Zn, Cd, and Ag) mean that INAA determinations presented here on heavy mineral concentrates do not add any insight into the potential for VMS style mineralization within the study area.

CONCLUSIONS

In part of the QUEST Project area, central BC, approximately 760 till samples have been collected where thick glacial deposits cover bedrock, hindering both bedrock mapping and mineral exploration programs. The study area occurs within the Quesnel terrane, and is dominated by middle to upper Triassic mafic volcanic rocks and volcaniclastic sedimentary rocks of the Nicola Group. The Mount Milligan Cu-Au porphyry deposit occurs just to the northwest of the study area in correlative rocks, part of a near linear, northwest-trending series of Cu±Mo deposits that occur within this terrane. Till geochemical data (clay and clay+silt) and heavy mineral grain count data and metal contents of the < 0.25 mm fraction, highlight four areas that warrant further work:

1) In the northwestern part of the study area, there is a large number of till samples with significantly anomalous Cu and Au contents (and coincident but less significant As and Ag anomalies). The underlying rocks are correlative with those that host the Mount Milligan Cu-Au porphyry deposit. Consistent with the potential for porphyry Cu-Au style mineralization, there are a number of showings associated with alkalic volcanic and porphyritic rocks. This area also has till samples elevated in Hf, REE, Th, Ti, Fe and V, reflecting Fe-rich alkalic igneous rocks in the underlying and up-ice bedrock.
2) In the northeastern part of the study area, there are Au, Cu, As, Ag, Sb and Cd anomalies in till occur near several precious and base metal vein showings and two small-scale past-producing Au (and Pt) placer mines.
3) In the east-central portion of the study area, till samples have elevated Zn, Cd and Bi contents, as well as high pyrite grain counts (up to 10 000 grains in a 10 kg sample). There are no known showings or mineralization in this part of the study area but the till geochemical results suggests there is potential for concealed VMS-type mineralization.
4) In the west-central portion and into the central portion of the study area, Hg values and elevated cinnabar grain counts suggest there is fault-associated Hg mineralization up-ice (i.e., to the southwest), perhaps similar to the Pinchi Lake mercury mine located to the west of the study area.

In these four areas increased till sample density could provide some insight into covered bedrock lithologies and the potential for metallic mineralization. Till sampling can become more challenging, however, as sample density increases appropriate sample material can be difficult to find and access to good sample sites can be limited. In such cases, prospecting (including an examination of clasts in drift) and trenching could be carried out to further test these areas.

ACKNOWLEDGMENTS

Geoscience BC provided the majority of funding for this project and the authors extend many thanks to C. Anglin and C. Sluggett for helping to make this project happen. The Mountain Pine Beetle (MPB) Program under the direction of C. Hutton (GSC, Natural Resources Canada) facilitated by Alain PLouffe provided funding for a portion of the geochemical analyses for samples taken in 2008. Alain Plouffe also arranged for the archiving of samples at the GSC. M. Casola, M. Dinsdale, K. Kennedy, V. Levson, J. McDonald, C. Pennimpede, S. Reichheld, I. Sellers and D. Vis provided able assistance in the field. A thorough review by T. Ferbey helped to greatly improve the manuscript.

REFERENCES

Armstrong, J. E., Crandell, D. R., Easterbrook, D. J. and Noble, J. B. (1965): Late Pleistocene stratigraphy and chronology in south-western British Columbia and north-western Washington; Geological Society of America Bulletin, v. 72, p. 321-330.

Averill, S. A. (2001): The application of heavy indicator mineralogy in mineral exploration with emphasis on base metal indicators in glaciated metamorphic and plutonic terrains. Geological Society Special Publications v. 185, p. 69-81.

BC Geological Survey (2010): MINFILE BC mineral deposits database; BC Ministry of Forest, Mines and Lands, URL <http://minfile.ca/> [August 2010].

Bobrowsky, P.T., Rutter, N.W. (1992): The Quaternary geologic history of the Canadian Rocky Mountains. Geographie physic et Quaternaire v. 46, p. 5–50.

Clague, J.J. (1989): Chapter 1: Quaternary geology of the Canadian Cordillera; *in* Quaternary Geology of Canada and Greenland, R. J. Fulton (ed.), Geology of Canada Series No. 1., p. 17-96.

Clague J.J., Ward B.C. (2011): Pleistocene glaciation of British Columbia. In Quaternary glaciations – extent and chronology, a closer look, Ehlers J, Gibbard PL, Hughes PD (eds), *Developments in Quaternary Science* **15**: 563–573.

Dreimanis, A., (1989): Tills: their genetic terminology and classification. In: Goldthwait, R. P. and Matsch, C. L. Eds.)*Genetic Classification of Glacigenic Deposits*. A.A. Balkema, Rotterdam.

Dilabio, R.N.W. (1990): Classification and interpretation of the shapes and surface textures of gold grains from till; *in* Current Research, Part C, Geological Survey of Canada, Paper 90-1C, p. 323–329.

Dostal, J., Gale, V. and Church, B.N. (1999): Upper Triassic Takla Group volcanic rocks, Stikine Terrane, north-central British Columbia: geochemistry, petrogenesis, and tectonic implications; Canadian Journal of Earth Sciences, v. 36, p. 1483–1494.

Dreimanis, A. (1989): Tills: their genetic terminology and classification; *in* Genetic Classification of Glacigenic Deposits, R.P. Goldthwait and C.L. Matsch (ed.), A.A. Balkema, Rotterdam, p. 17–83.

Erdmer, P., Moore, J.M., Heaman, L., Thompson, R.I., Daughtry, K.L. and Creaser, R.A. (2002): Extending the ancient margin outboard in the Canadian Cordillera: record of Proterozoic crust and Paleocene regional metamorphism in the Nicola horst, southern British Columbia; Canadian Journal of Earth Sciences, v. 39, p. 1605–1623.

Ferbey, T. Levson and V. M. (2010): Evidence of Westward Glacial Dispersal Along a Till Geochemical Transect of the Copper Star Cu+/-Mo+/-Au Occurrence, West-central British Columbia; BC Ministry of Energy and Mines Open File 2010-04

Ferbey, T. Levson, V.M. and Lett, R.E. (2012): Till Geochemistry of the Huckleberry Mine Area, West-Central British Columbia (NTS 093E/11); BC Ministry of Energy and Mines Open File 2012-02

Franklin, J.M., Lydon, J.W. and Sangster, D.F. (1981): Volcanic-associated masive sulfide deposits; Economic Geology, 75th Anniversary, p. 485–627.

Galley, A.G., Hannington, M. and Jonasson, I. (2007): Volcanogenic massive sulfide deposits; *in* Mineral Deposits of Canada: A Synthesis of Major Deposit-Types, District Metallogeny, the Evolution of Geological Provinces, and Exploration Methods, W.D. Goodfellow (ed.), Geological Association of Canada, Special Publication no. 5, p. 141–161.

Hall, G.E.M., Parkhill, M.A. and Bonham-Carter, G.F. (2003): Conventional and selective leach geochemical exploration methods applied to humus and B horizon soil overlying the Restigouche VMS deposit, Bathurst Mining Camp, New Brunswick; *in* Massive Sulphide Deposits of the Bathurst Mining Camp, New Brunswick, and Northern Maine, W.D. Goodfellow, S.R. McCutcheon and J.M. Peter (ed.), Economic Geology Monograph 11, p. 763–782.

Hoffman, E.L. (1992): Instrumental neutron-activation in geoanalysis; Journal of Geochemical Exploration, v. 44, p. 297–319.

Holland, S. S., (1976): Landforms of British Columbia – a physiographic outline; British Columbia Ministry of Energy, Mines and Petroleum Resources, Bulletin 48, p. 138.

Jackson Jr., L.E., Clague, J.J. (Eds.), (1991): The Cordilleran Ice Sheet, In: Geographie physique et Quaternaire. 45, 261–377.

LeFort, Darren; Hanley, Jacob; Guillong, Marcel. (2011): Subepithermal Au-Pd mineralization associated with an alkalic porphyry Cu-Au deposit, Mount Milligan, Quesnel Terrane, British Columbia, Canada. Economic Geology and the Bulletin of the Society of Economic Geologists v. 106, p. 781-808.

Levson, V.M. (2001): Regional till geochemical surveys in the Canadian Cordillera: sample media, methods and anomaly evaluation; *in* Drift Exploration in Glaciated Terrain; McClenaghan, M.B, Bobrowsky, P.T., Hall, G.E.M. and Cook, S.J., Editors, The Geological Society, Special Publication No. 185, p. 45-68.

Levson, V.M. and Giles, T.R. (1997): Quaternary geology and till geochemistry studies in the Nechako and Fraser Plateaus, central British Columbia *in* Interior Plateau Geoscience Project: Summary of Geological, Geochemical and Geophysical Studies; Diakow, L.J., Metcalfe, P. and Newell J., Editors, British Columbia Geological Survey, Paper 1997-2, p. 121-145.

Leybourne, M.I., Boyle, D.R. and Goodfellow, W.D. (2003): Interpretation of stream water and sediment geochemistry in the Bathurst Mining Camp, New Brunswick: applications to mineral exploration; *in* Massive Sulphide Deposits of the Bathurst Mining Camp, New Brunswick, and Northern Maine, W.D. Goodfellow, S.R. McCutcheon and J.M. Peter (ed.), Economic Geology Monograph 11, p. 741–761.

Logan, J. M., Schiarizza, P., Struik, L. C., Barnett, C., Nelson, J. L., Kowalczyk, P., Ferri, F., Mihalynuk, M. G., Thomas, M. D., Gammon, P., Lett, R., Jackaman, W., and Ferbey, T. (2010): Bedrock Geology of the QUEST map area, central British Columbia; . *Geoscience BC Report*

2010-5, British Columbia Geological Survey Geoscience Map 2010-1 and Geological Survey of Canada Open File 6476.

Mathews, W.H. (1986): Physiographic map of the Canadian Cordillera; Geological Survey of Canada, “A” Series Map 1710A, scale 1:5 000 000.

McClenaghan, M.B. (2005): Indicator mineral methods in mineral exploration; Geochemistry: Exploration, Environment, Analysis, v. 5, p. 233–245.

McClenaghan, M.B., Ward, B.C., Kjarsgaard, I.M., Kjarsgaard, B.A., Kerr, D.E. and Dredge, L.A. (2002): Indicator mineral and till geochemical dispersal patterns associated with the Ranch Lake kimberlite, Lac de Gras region, NWT, Canada; Geochemistry: Exploration, Environment, Analysis, v. 2, p. 299–320.

Nicholson, K., and Eley, M. (1997): Geochemistry of manganese oxides; metal adsorption in freshwater and marine environments. Geological Society Special Publications v. 119, p. 309-326.

Parkhill, M.A. and Doiron, A. (2003): Quaternary geology of the Bathurst Mining Camp and implications for base metal exploration using drift prospecting; *in* Massive Sulphide Deposits of the Bathurst Mining Camp, New Brunswick, and Northern Maine, W.D. Goodfellow, S.R. McCutcheon and J.M. Peter (ed.), Economic Geology Monograph 11.

Patchett, P.J. and Gehrels, G.E. (1998): Continental influence on Canadian Cordilleran terranes from Nd isotopic study, and significance for crustal growth processes; Journal of Geology, v. 106, p. 269–280.

Paulen, R.C. and Bobrowsky, P.T. (2003): Multiphase flow of Late Wisconsin ice in the Quesnel Highlands: piecing together discordant ice flow indicators. Program with abstracts, vol. 28, p. 132, 2003 GAC-MAC-SEG, Vancouver.

Plouffe, A. (1997): Ice flow and late glacial lakes of the Fraser Glaciation, central British Columbia*; in* Current Research 1997-A, Geological Survey of Canada, p133-143.

Plouffe, A. (2000): Quaternary geology of the Fort Fraser and Manson River map areas, central British Columbia Geological Survey of Canada, Bulletin 554, p. 62.

Ross, G.M., Patchett, P.J., Hamilton, M., Heaman, L., Decelles, P.G., Rosenberg, E. and Giovanni, M.K. (2005): Evolution of the Cordilleran orogen (southwestern Alberta, Canada) inferred from detrital mineral geochronology, geochemistry, and Nd isotopes in the foreland basin; Geological Society of America Bulletin, v. 117, p. 747–763.

Sacco, D.A., Ward, B.C., Maynard, D., Geertsema, M. and Reichheld, S. (2010): Terrain mapping, glacial history and drift prospecting in the northwest corner of Mcleod Lake map area (part of NTS 093J), central British Columbia; *in* Geoscience BC Summary of Activities 2009, Geoscience BC, Report 2010-1, p. 33-42.

Sander Geophysics Limited (2008): Airborne gravity survey, Quesnellia Region, British Columbia; Geoscience BC, Report 2008-08, 121 p.

Smith, A.D., Brandon, A.D. and Lambert, R.S. (1995): Nd-Sr isotope systematics of Nicola Group volcanic rocks, Quesnel terrane; Canadian Journal of Earth Sciences, v. 32, p. 437–446.

Struik, L.C. (1994): Geology of the Mcleod Lake map area (93J), British Columbia; Geologic Survey of Canada, Report: 2439, 18 pp.

Taylor BE (2007) Epithermal gold deposits In: Goodfellow WD (ed) Mineral Resources of Canada: A Synthesis of Major Deposit-types, District Metallogeny, the Evolution of Geological Provinces, and Exploration Methods. pp 113-139.

Tipper, H.W. (1971): Glacial geomorphology and Pleistocene history of central British Columbia; Geologic Survey of Canada, Bulletin 196, 89 p.

Ward, B. C., Geertsema, M., Telka, A., and Mathewes, R. W. (2008): A paleoecological record of climatic deterioration from middle to late Wisconsinan time on the Interior Plateau of British Columbia, Canada. 33rd International Geological Congress, August 6–14, 2008, Oslo, Norway.

Ward, B., Maynard, D., Geertsema, M. and Rabb, T. (2009): Ice-flow history, drift thickness and drift prospecting for a portion of the QUEST Project area, central British Columbia (NTS 093G, H [west half], J); *in* Geoscience BC Summary of Activities 2008, GeoscienceBC, Report 2009-1, p. 25–32.

Ward, B.C., Leybourne, M.I. and Sacco, D.A. (2011): Drift prospecting within the QUEST project area (NTS 093J): Mineral potential for porphyry Cu-Au, VMS, and Au-Cu Veins; *in* Geoscience BC Summary of Activities 2011, Geoscience BC, Report 2011-1, p. 73-96.

Ward, B.C., Leybourne, M.I. and Sacco, D.A. (2012): Heavy mineral analysis from till samples within the QUEST Project Area, central British Columbia (NTS 093J); *in* Geoscience BC Summary of Activities 2012, Geoscience BC, Report 2012-1, p 69-78.